BRITISH GEOLOGICAL SURVEY
Natural Environment Research Council

Mineral Reconnaissance Programme

Report No. 95

Mineral reconnaissance at Menear, St Austell, Cornwall

Geochemistry and Geology
K E Beer BSc CEng FIMM
B C Tandy MSc

Geophysics
G S Kimbell BSc

A report prepared for the Department of Trade and Industry

Keyworth, Nottinghamshire 1988

Contents:

SUMMARY

Geochemical soil sampling shows no evidence for a continuation of the Menear stockwork tin mineralisation beyond the eastern rim of the old openwork, though there may be some extension westwards below areas of recent housing development. Elevated levels of tin in soils are indicated to the north of Wheal Eliza with above average values of copper and zinc immediately to the south, over the site of that mine; VLF-EM anomalies delineate several possible mineral veins in this area. None of these metals is present at concentrations likely to interest prospecting companies.

INTRODUCTION

Menear Pit [SX 032541], also known as Minear Downs Mine and probably as Buckey Pit, is a former opencast working for cassiterite situated 2km NE of St. Austell railway station, close to the edge of new housing estates at Boscoppa. Until recently the pit was an open quarry some 230m long (east-west), 70m wide and up to 50m deep.

The tin deposit was a stockwork emplaced within metamorphosed Meadfoot Group, Lower Devonian, slates some 400m from the St. Austell granite contact. Dines (1956) describes the mineralisation as "numerous more or less parallel tin-bearing joints, up to an eighth of an inch wide and 2 to 12 inches apart". These trend almost east-west and dip steeply north. A so- called "lode" (Foster, 1878) was merely a discontinuous zone of intense tourmalinisation. At the western end of the pit a shaft, of unknown depth, proved the mineralisation to continue below the floor.

The overall grade is not known with any certainty but is presumed to have been about 4lb. of black tin per ton (i.e. about 0.125%Sn). At this grade the 1.5 million tonnes of rock extracted from the pit should have yielded some 1,950 tonnes of tin metal. Production records are obviously incomplete and total only 976 tons of tin concentrate, about 700 tonnes of metal. The pit seems to have been last worked in 1915.

According to Dines (1956), the pattern of mineralisation in this part of the aureole indicates the presence of a small emanative centre encompassing Menear and the adjacent mines. The surrounding area, therefore, should constitute a prime target for further investigation, but westwards and southwards there is urban development, while northwards is the granite contact just inside which lie the stockworks of Carclaze and the east-west veins of Garker and Pentruff. The best prospects for examination therefore appear to be to the east and south-east of Menear Pit; in the openwork it seemed that the stockwork weakened eastwards with the fewer remaining veins becoming somewhat wider and stronger in that direction. It was therefore thought possible that there might be further mineral structures in the ground along strike from the pit, immediately to the north of Boscoppa Mine (Fig. 1) and, perhaps, within that former mine sett. This potentiality was examined by geochemical soil sampling (Fig. 2) and by geophysical traverses (Fig. 24) using a combination of very low frequency (VLF), resistivity (RES) and induced potential (IP) methods.

GEOCHEMICAL SAMPLING

Traverses were aligned roughly north-south to cross the general vein direction at about right angles. They were positioned, within the constraints imposed by field hedges, to examine the apparently unworked areas east of Menear Pit and between Boscoppa Mine and Wheal Eliza. One short traverse was laid out to the north-west of the pit; in this, soil samples were augered at stations 50m apart, elsewhere the station interval was 20m. Wherever possible soil samples were taken from a depth of about 1m, in the "C" horizon. For the most part this was a slightly silty yellowish or brownish clay with some samples of a more reddish ferruginous character.

The soils were oven dried, disaggregated and dry sieved at 80mesh BSS. Sub-samples of the undersize fraction were ground finer and used for geochemical analysis in analytical laboratories at Gray's Inn Road, London. In order to cover the full range of elements desired, three analytical techniques were employed. Co, Cu, Ni and Zn were determined by atomic absorption spectrometry (AAS), B, Ba, Be, Cr, Fe, Mn, Mo, Pb, Sn, V, Y and Zr by optical emission spectrometry (OES) and Ba, Ca, Ce, Fe, Mn, Sb. Sn, Ti and W by X-ray fluorescence analysis (XRF); four elements are repeated in the last two methods. As a broad check upon both sampling and analysis a total of twenty duplicate samples were collected and analysed.

GEOCHEMICAL RESULTS

In Appendices 1 to 4 the complete analytical results are tabulated by method. From these, basic statistics were calculated for all the elements and cumulative distribution plots prepared for the economically interesting base metals and associated volatile elements. This information is summarised in Table 1 and the distribution plots comprise Figures 3 to 13. Element-in-soil maps for the most significant elements are reproduced in Figures 14 to 23.

Table 2 compares the analyses of duplicate samples from twenty sampling sites. They are not splits from single samples but are separate samples from two close-spaced auger holes. The difference between the two values for each element is quoted as a percentage of the lower value. It may be anticipated that some variation in elemental levels will arise from slight mineralogical differences between separate samples, from sub-sampling of unclassified granular material and from statistical drift in automated analytical measurements. As a rule of thumb it was assumed that duplicate variance of less than 25% signified good reproducability, 25-50% represented good agreement and less than 100% was workably acceptable duplication.

On this basis the essential and stable soil elements (Ba, Ca, Cr, Fe, Mn and Ti) indicate that sampling duplication is good in almost every case and, it follows, that the XRF method provides reproducable results. Wider spreads are exhibited by some elements, notably those contained in refractory particulate minerals - Ce, Sn, Y and Zr, for instance. But boron, contained largely in tourmaline, shows good repeatability.

Table 1. Summary of geochemical statistics

Fe in percent, remainder in ppm
n = 240 except for W, for which it is 232

ELEMENT	RANGE	MEAN	S.D.	MEDIAN	ANOMALOUS SETS
Atomic absorption spectrometry					
Co	0-40	10.4	6.8	10	
Cu	0-90	35.0	14.5	30	>43(25%)
Ni	0-45	18.9	8.5	20	
Pb	10-110	29.4	12.6	30	>44(2.5%)
Zn	10-120	45.1	24.5	40	>96(6%)
Optical emission spectrometry					
B	10*-2300	849.5	369.1	872	>1230(8%); >1600(4.8%)
Ba	100*-615	337.4	68.5	333	Ill defined
Be	1.0*-9.0	2.48	0.87	2.3	
Cr	19-244	102.5	23.6	101	
Fe	1.42-5.86	3.632	0.726	3.63	
Mn	50*-1400	298.5	331.6	143	
Mo	1.0*-24.6	3.29	11.64	1.9	>6.1(8%);>9.0(2%)
Nb	20*-52	14.1	11.9	20	
Sn	5*-517	139.7	96.0	110	>135(42%); >270(11%)
V	33-242	128.8	23.8	126	
Y	5.3-41.5	25.35	3.98	24.9	
Zr	20*-660	406.1	79.3	397	
X-ray Fluorescence Spectrometry					
Ba	63-518	370.8	47.8	370	>400(15%)
Ca	300-3880	1473	589	1450	
Ce	7-151	62.48	14.53	62	
Fe	2.474-7.825	5.4484	0.8211	5.498	
Mn	60-1270	334	287	190	
Sb	0-16	4.88	3.58	5	>9.2(10%)
Sn	39-470	149.2	83.5	131	>170(36%)
Ti	4160-8590	7220	474	7230	
W	4-32	12.43	3.87	12	>19(3%)

* Detection limit; values below this level are recorded as zero

Two other features stand out. Firstly, there is a considerable divergence between OES and XRF percentages for the same element and within OES results for individual elements. Secondly, some of the persistently high percentages are found among elements where the absolute values are low and the determination intervals relatively large (eg. Be, Co, Pb, Ni and Sb), though Cu and Zn, which fall in this category, show better repeatablity.

In the succeeding paragraphs brief individual consideration is given only to those elements for which cumulative frequency plots were prepared, and these comments amplify the distributions of anomalous levels plotted in Figs. 14 to 23. Because the results are derived from three widely differing analytical techniques, no attempt has been made to prepare correlation coefficient tables. It has not been

established, therefore, to what extent the more mobile elements (especially copper and zinc) may have been redistributed by adsorption on, or co-precipitation with, hydrated secondary iron and manganese oxides.

Copper. At 43ppm the break of slope in the cumulative frequency plot (Fig. 3) reflects a level of copper concentration which accords well with values recorded widely throughout south-west England. In an area where copper ores were actively mined it is not surprising that a quarter of the soil samples prove to be anomalous for that element. In Fig. 14 these higher copper values are seen to be concentrated in

Table 2. Comparison of repeat samples; percentage difference

Samples	7	29	37	45	57	67	78	98	105	109
XBS	223	224	225	226	227	228	229	230	231	232
Atomic Absorption Spectrometry										
Co	---	100	100	0	50	0	100	0	300	0
Cu	---	0	25	50	0	0	20	13	11	20
Ni	300	33	67	33	150	0	33	0	0	100
Pb	0	33	50	50	50	0	100	0	0	50
Zn	0	0	33	33	0	50	25	0	0	0
Optical Emission Spectrometry										
B	5	8	43	46	7	30	46	21	10	7
Ba	30	19	10	6	31	35	38	17	49	16
Be	12	0	24	31	14	105	90	47	32	21
Cr	34	36	3	8	15	44	9	11	12	46
Fe	1	22	48	39	12	51	47	35	29	1
Mn	51	5	20	13	146	159	37	38	30	20
Mo	53	50	129	119	1347	107	108	89	69	---
Nb	21	---	---	---	25	---	0	15	---	---
Sn	75	20	89	13	129	11	28	40	14	14
V	49	9	20	63	19	54	3	40	32	3
Y	2	37	5	7	46	2	35	84	8	18
Zr	11	20	47	85	7	37	40	27	13	21
X-ray Fluorescence Spectrometry										
Ba	11	9	4	1	1	7	8	2	3	2
Ca	22	2	24	16	4	11	6	1	32	8
Ce	13	5	2	4	8	21	12	4	18	39
Fe	19	3	1	11	7	11	6	1	3	4
Mn	0	0	7	15	12	0	9	10	23	2
Sb	0	---	700	71	100	---	100	200	500	33
Sn	151	20	21	31	4	4	6	16	19	11
Ti	7	1	4	1	0	1	1	3	0	0
W	WC	15	50	44	31	11	21	0	7	13
Gravimetric										
LOI	4	70	54	17	49	15	50	179	4	1

--- indicates one of the determinations below detectable level
WC indicates one of the samples crushed in a tungsten carbide mill

Table 2 (cont.).

Samples	126	133	142	156	165	178	186	195	209	211
XBS	233	234	235	236	237	238	239	240	220	221
Atomic Absorption Spectrometry										
Co	100	100	0	100	33	50	50	100	100	150
Cu	0	25	43	14	11	0	0	0	22	0
Ni	0	100	100	50	200	100	100	300	200	75
Pb	50	0	200	0	33	0	0	0	33	33
Zn	50	33	50	0	13	0	0	13	0	0
Optical Emission Spectrometry										
B	21	80	9	1	11	45	74	38	11	29
Ba	96	5	26	40	27	26	12	7	80	3
Be	6	128	5	32	5	76	133	76	25	43
Cr	43	3	45	21	54	9	5	1	14	23
Fe	10	28	18	20	10	14	32	41	21	31
Mn	133	110	13	51	18	29	113	58	7	35
Mo	440	40	80	---	---	---	---	262	---	---
Nb	---	---	9	*	---	*	*	---	*	---
Sn	54	19	30	144	27	53	56	91	49	160
V	87	1	66	15	92	41	49	35	15	20
Y	15	39	16	27	45	5	2	5	15	4
Zr	10	6	27	13	23	37	54	18	50	36
X-ray Fluorescence Spectrometry										
Ba	1	5	2	3	7	6	1	0	2	5
Ca	20	9	5	23	3	26	39	8	11	4
Ce	31	40	0	54	42	7	16	13	11	35
Fe	3	2	10	2	5	2	4	1	9	1
Mn	10	5	14	0	12	3	10	6	7	10
Sb	33	17	67	100	---	---	700	250	150	250
Sn	8	7	4	32	3	4	15	21	16	46
Ti	2	1	0	2	1	1	1	1	1	1
W	23	11	6	0	43	0	0	33	0	29
Gravimetric										
LOI	16	30	39	18	35	32	136	2	26	27

--- indicates one of the determinations below detectable level
* indicates both the determinations below detectable level

the south-eastern part of the area, between Boscoppa Mine and Wheal Eliza. From Dines' (1956) limited description it seems that the veins in this area are essentially tin-bearing and this westward spread of anomalous copper is somewhat unexpected, therefore, and may betoken the presence of a mixed ore zone. The distribution pattern does not correlate closely with that of any other ore metal.

Lead. Determination of lead by AAS may be less accurate than by XRF but avoids the problems of energy peak interference between Pb and Sn, thus giving more meaningful results. Most of the values fall within a "background" population which extends to the rather high level of

44ppm. Only 9 samples exceed this value and all but two of these derive from scattered sites in the eastern part of the survey area (Fig. 15). There is no suggestion of a northerly trend to these anomalies and, consequently, they cannot be interpreted as indicating the presence of mineralised crosscourses. The central of the three eastern anomalies correlates closely with the trend of the western part of the West Wheal Eliza adit level (Fig. 1) but it is uncertain whether this working actually follows a mineralised structure. There is no correspondence between the distribution pattern of Pb and that of its usual associates, Cu, Zn and Ba.

Zinc. The cumulative frequency plot for Zn is somewhat less than satisfactory and may be interpreted as showing three populations rather than the two defined in Fig. 5. In any event the most anomalous values represent only a few percent of the total samples and these are concentrated entirely in the extreme south-east of the surveyed area, immediately west of Wheal Eliza and north of West Wheal Eliza. There is no close correlation with the distribution of other elements nor is there any clear relationship to the known and worked mineral veins.

Boron. At least three distribution populations are represented in the cumulative frequency plot for B (Fig. 6), and it is tempting to regard these as reflections of separate phases of tourmaline formation during magmatic emplacement and hydrothermal mineralisation. Only the most anomalous set, representing about 5% of the total, has been plotted on the distribution map (Fig. 17). The high value samples are scattered through the traverses with no apparent pattern, except perhaps in the extreme west. Here, north-west of the Menear Pit, all the samples show high B contents and this feature may reflect the closeness of this traverse line to the granite margin. It might be suggested that these elevated B levels are spatially associated with stockwork hypothermal tin mineralisation, but farther east there is no obvious relationship between B anomalies and tin veining.

Molybdenum. This element also yields a complex cumulative frequency plot (Fig. 8) but, on the basis of Mo levels from other sites in SW England, populations with more than 6.1ppm Mo have been taken as anomalous. The resulting distribution map shows a meaningless scatter of anomalies across the whole study area with no relationship to any other ore element.

Barium. A cumulative frequency plot of Ba values determined by the OES method (Fig. 7) reveals no clear separation of population sets, but the equivalent plot for XRF values (Fig. 10) divides the samples into three groups. A low value group is strongly defined with the remainder almost, but not quite, log-linear; a minor change of slope separates an anomalous population above 400ppm. When plotted (Fig. 20) these high values display a strange distribution pattern, developed predominantly in the south-east of the study area but bearing little or no relation to recorded vein locations in the three surrounding mines. Also, there is no correlation with the distribution patterns for any of the ore elements. It is presumed, therefore, that the Ba-in-soil values are a direct reflection of contents in the underlying altered Devonian sediments.

Tin. Cumulative plots of Sn determined by OES and XRF (Figs. 9 & 12) produce distribution curves which, though complex, are basically

similar. The OES plot seems to define an upper anomalous population with Sn in excess of 270ppm, and containing about 10% of the samples, with another break of slope at 135ppm Sn. In the case of the XRF results these two groups are less obviosly separable and the anomalous population is taken as that in excess of 170ppm, about one-third of the total number. This value and the lower OES figure are adopted for distribution plots of Sn anomalies (Figs. 19 & 22).

Although there is variation of detail, in essence these two maps exhibit similar distribution patterns. Anomalous Sn values over the full length of the traverse west of Menear Pit apparently finger out immediately east of the openwork. To the east this is succeeded by a zone almost devoid of anomalous soils. Farther east the Sn anomaly begins again near the northern end of the XBS77-105 traverse and it intensifies eastwards. It seems from this pattern that there is no direct connection, at least at surface elevations, between the stockwork tin mineralisation worked in Menear Pit and the cassiterite veins of Boscoppa Mine and the Wheal Elizas. It is interesting to note that there is only partial overlap of the Cu and Sn anomalies and this may suggest that only in the south is the "tin zone" beginning to plunge beneath that of copper.

Antimony. The cumulative frequency plot for Sb divides cleanly into three sections of which the anomalously high one commences at 9.2ppm and represents just over 10% of the total samples (Fig. 11). When related to the traverse sites (Fig. 21), the 27 anomalous samples are widely scattered to the east of the openwork but there are none in the traverse north-west of the pit. A series of lines can be drawn around or through the anomalous points but they fail to produce a consistent pattern.

Tungsten. The W results produce a relatively simple cumulative frequency plot in which there is an anomalous population at values above 19ppm. This set represents a mere 3% of the total and, accordingly, tungsten can be immediately dismissed as a significant ore metal in the Menear area. Their six sites (Fig. 23) are scattered and are seemingly unrelated to the distribution of the other metals.

GEOPHYSICAL METHODS

Surveys were undertaken to investigate whether the Menear stockwork and the mineral veins in the area have a geophysical signature which would allow the mapping of their possible extensions. Recorded Sn concentrations are low and unlikely to be detectable directly by geophysical methods, but the more fractured rocks associated with the stockwork and veins may have an electrical resistivity significantly lower than surrounding rocks because of a higher water content. The Very Low Frequency electromagnetic (VLF-EM) method was employed to detect such conductive zones. Measurements of the in-phase and out-of-phase components of the vertical secondary magnetic field were made at 10m intervals along survey traverses using Geonics EM16 equipment tuned to the Maine (NAA) VLF transmitter which, at the time of the survey, broadcast on a frequency of 17.8 kHz. On some traverses VLF-R surveys were conducted, which entail measuring the ratio and

phase angle between the orthogonal, horizontal electric and magnetic field components; an apparent resistivity is calculated from the ratio measurement and the phase angle can give an indication of the variation of resistivity with depth.

Some resistivity and induced polarisation (IP) trials were made using Huntec MkIII equipment. A colinear dipole-dipole array was used with 50m dipoles and dipole centre separations of 100m (n=2) to 300m (n=6); using the criterion of Edwards (1977), the maximum depth of investigation with these parameters is of the order of 75m. Chargeabilities were derived from the time integral of the voltage decay curve between 240ms and 1140ms after the termination of a 2s current pulse.

The locations of the geophysical traverses and the methods employed on them are shown in Figure 24. Geochemical soil sampling was conducted on or near parts of lines A to I; the other traverses were solely for additional geophysical infill.

GEOPHYSICAL RESULTS

VLF-EM surveys.

The in-phase VLF-EM data have been filtered using the Fraser operator (Fraser, 1969), which converts downward inflections across conductors to maxima, and the positive values plotted on a plan of the survey lines (Figure 25). A particular problem in this area is the interference from electrical transmission lines and, to a lesser extent, from grounded fences and buried pipes. Only those VLF-EM features which are interpreted as having a geological cause are shown in Figure 25. There are gaps in the data coverage where "man-made" anomalies swamp any geological effects.

Two power lines influence the region immediately east of the Menear Pit, but from the data that can be obtained it appears unlikely that there is a strong VLF-EM response directly over an eastward projection of the stockwork: similarly, there is not a strong response on line A over its western projection. Elsewhere, however, a number of approximately E-W trending linear VLF-EM anomalies are considered most likely to be related to fracture zones: these are labelled 1 to 5 in Figure 25. Such fracture zones may be mineralised.

Anomaly 1 lies to the north of the geochemical survey, so its mineral potential cannot be assessed. Anomaly 2 passes just to the north of the Menear stockwork; although it cannot be unambiguously identified on line H, because of interference from man-made sources, there does appear to be a correlation between the eastern end of this feature and slightly higher concentrations of Cu and Pb in soils (Figures 14 & 15). Anomalies 3, 4 and 5 lie in the area between Boscoppa Mine and Wheal Eliza (Figure 1). The first two may reflect eastward extensions of veins worked in Boscoppa, although there is a disparity in strike directions and no clear evidence of a VLF response over the known vein outcrops. Conductive material in a nearby spoil tip may have influenced the amplitude of anomaly 3 on line G. Anomaly 5 aligns well with a westward extension of the veins mined in Wheal Eliza. There is a correlation between anomalies 3, 4 and 5 and zones of high Sn in soils (Figures 19 & 22), supporting the hypothesis that the VLF-EM anomalies are related to mineral veins.

Resistivity and IP surveys.

Some resistivity (dipole-dipole and VLF-R) and IP trials were carried out over lines immediately to the east of Menear Pit (Figure 24). Results from line B were much distorted by the influence of power lines and fences, but more satisfactory data were obtained on lines C and C' farther to the east.

Resistivity and IP pseudosections for line C' are shown in Figure 26. A relatively resistive zone is centred on 250N and another on 500N. The latter appears to be overlain by a more conductive layer (possibly a weathering phenomenon) evident at the n=2 and n=3 dipole separations. The projection of the Menear stockwork intersects line C' in the zone of transition from higher to lower shallow apparent resistivities. At wider dipole separations the stockwork projection coincides with slightly lower apparent resistivities than are found in the highs to the south and north, possibly because of a higher concentration of fractures in this zone. This possibility might merit further investigation, although the geochemical results suggest that, even if the system of fractures associated with the Menear stockwork does extend into this area, Sn values are likely to decrease significantly.

There is a general positive correlation between apparent resistivity and chargeability on line C' (Figure 26). This is probably because the more resistive rocks have a smaller fluid content, so a greater proportion of the current flows through the rock matrix, and any mineral grains it contains, than is the case with more fractured or weathered rocks.

The apparent resistivities measured by the VLF-R method on line C show a similar pattern to those measured at smaller dipole spacings with the dipole-dipole array on line C': an apparent resis- tivity high is centred in the southern half of the line with a trans- ition to lower values in the northern half (Figure 27). The apparent skin depth (an indicator of depth of exploration) varies between about 30m and 100m respectively at the sites of lowest and highest apparent resistivity. Observed phase angles are all less than 45 degrees, and inversion of the VLF-R data suggests this is due to an approximately 2m thick soil or head layer with a resistivity of the order of 100 ohm metres. The apparent resistivies are lower than those measured by the dipole-dipole survey because of the greater influence of the relatively conductive soil layer on the VLF-R measurements. An underlying slight increase in phase angle towards the northern half of the line indicates that the broad northward resistivity decrease occurs in the bedrock rather than in the soil layer.

Shorter wavelength variations are superimposed on the long wavelength VLF-R trends. Some of these are simply "noise" due to measurement inaccuracies (the measurement is made by tuning to an audio null which was diffuse at some sites), but others are likely to have a geological cause. For example, the local apparent resistivity low at 370N is associated with VLF-EM anomaly 2 (Figure 25) and is interpreted as the response to a narrow conductive fracture zone which is not well resolved by the dipole-dipole survey; a local phase angle minimum is observed over this feature, as theory predicts (Hjelt and

others, 1985). A local apparent resistivity minimum at 300N lies along the projection of the Menear stockwork, but the amplitude of this feature is not significantly greater than the noise level and in this case there is no clear supporting VLF-EM evidence. The local apparent resistivity high at around 400N may correspond to the top of the resistive zone detected at 500N on line C' (Figure 26); the dipole-dipole method resolves this feature more clearly because of its better vertical resolution and (at this site) depth penetration.

CONCLUSIONS

The soil geochemistry has shown that the low-grade stockwork tin mineralisation formerly worked in the Menear Pit was fully developed eastwards by the openwork and has no extension immediately to the east of the pit. Reports and field observations suggest that in this direction the stockwork veinlets bunch together and may begin to form discrete veins but, if this be so, the geochemistry indicates that such mineralisation is not continuous with the cassiterite veins of Boscoppa Mine, Wheal Eliza and West Wheal Eliza which lie a short distance to the east.

The only other ore metal which exhibits a meaningful distribution pattern of anomalies is copper. This element is concentrated in the soils to the south-east of the study area and in part overlaps the anomalous tin area. It is possible that in this area of overlap the veins carry mixed ores of cassiterite and copper sulphides; on the other hand the presence of both ore metals in anomalous quantities may imply proximity to the upper boundary of the "tin zone", a suggestion in accord with Dines' recognition of an emanative centre in the Menear area (1956, p.552).

Despite a high level of interference from man-made sources, several linear VLF-EM anomalies were detected which show an apparent correlation with geochemical anomalies, and which may thus be due to fracture zones containing mineralisation. There was no clear VLF-EM response over possible extensions of the Menear stockwork, although a dipole-dipole traverse indicates slightly lower apparent resistivities to the east of the stockwork, probably reflecting those closely-spaced fractures which extend into this region.

Although the geochemistry clearly defines the existence of tin and copper mineralisation around and immediately west of the Wheal Elizas, and tin mineralisation north-west of the Menear Pit, none of the anomalies can be easily extended for any distance because of building development or contamination from china clay workings. The Sn and Cu values reported from the soils are generally of a level which would not greatly encourage the mineral exploration groups, especially in view of the problems presented to possible mining. The best prospects for improved grades may lie in depth but it is doubtful whether the area offers enough potentially mineralised structures to make exploration an economic attraction.

ACKNOWLEDGEMENTS

These investigations were greatly assisted by the generous co-operation of the local landowners and of English China Clays, who own

the Menear Pit. Various Geological Survey colleagues have aided in the preparation of data for this report, not least the members of the Analytical Chemistry Unit who carried out all the analyses.

REFERENCES

DINES, H.G. 1956 "The metalliferous mining region of south-west England". Memoirs of the Geological Survey of Great Britain, 2 vols., 795pp. London: HMSO.

EDWARDS, L.S. 1977 "A modified pseudosection for resistivity and IP". Geophysics, Vol. 42, pp. 1020-1036.

FOSTER, C. Le N. 1878 "On some tin stock works in Cornwall". Quarterly Journal of the Geological Society, Vol. 34, pp. 654-659.

FRASER, D.C. 1969 "Contouring of VLF-EM data". Geophysics, Vol. 34, pp. 958-967.

HJELT, S.E., KAIKKONEN, P. and PIETILA, R. 1985 "On the interpretation of VLF resistivity measurements". Geoexploration, Vol. 23, pp. 171-181.

APPENDIX 1 Soil analyses, AAS.

All in ppm

Sample XBS	Co	Cu	Ni	Pb	Zn	Sample XBS	Co	Cu	Ni	Pb	Zn
0001	0	5	0	30	20	0050	10	20	5	20	20
0002	0	5	5	25	20	0051	10	35	10	20	20
0003	0	10	5	30	20	0052	10	30	15	30	30
0004	0	20	10	30	20	0053	10	25	15	30	30
0005	0	25	10	30	20	0054	10	25	15	30	30
0006	0	20	10	30	20	0055	15	35	20	30	30
0007	0	10	5	30	20	0056	15	20	20	30	30
0008	0	20	20	30	30	0057	15	20	10	30	30
0009	0	25	25	40	40	0058	10	20	10	30	30
0010	0	20	20	40	40	0059	10	10	10	20	20
0011	0	30	15	30	30	0060	10	25	10	30	20
0012	0	20	20	40	40	0061	10	20	10	30	20
0013	0	25	15	40	30	0062	10	30	10	30	40
0014	0	50	15	40	30	0063	10	15	15	20	30
0015	0	20	15	40	30	0064	10	20	10	20	20
0016	5	20	15	40	30	0065	10	30	15	30	30
0017	0	35	15	110	50	0066	10	30	10	30	20
0018	0	20	15	20	40	0067	10	30	10	30	30
0019	0	15	10	30	30	0068	0	30	10	20	20
0020	0	20	10	30	40	0069	10	30	10	30	20
0021	0	20	10	30	40	0070	10	40	10	20	20
0022	0	15	10	20	20	0071	10	30	10	30	50
0023	0	20	10	30	20	0072	10	20	10	30	20
0024	0	30	10	30	30	0073	10	30	10	30	30
0025	0	20	15	40	20	0074	10	55	10	30	20
0026	0	30	10	30	20	0075	10	45	10	30	30
0027	10	50	20	40	30	0076	10	40	10	20	20
0028	5	30	10	30	20	0077	20	25	15	30	40
0029	5	20	15	40	40	0078	20	30	20	40	50
0030	5	25	20	40	40	0079	20	30	20	40	50
0031	10	25	20	40	50	0080	20	30	20	40	60
0032	10	30	20	40	50	0081	20	30	20	40	60
0033	10	20	20	40	40	0082	20	30	20	40	60
0034	5	25	20	40	30	0083	20	30	20	40	50
0035	5	25	20	40	40	0084	10	30	10	30	30
0036	10	20	20	20	40	0085	20	30	15	50	40
0037	5	25	15	20	40	0086	20	30	15	30	40
0038	5	20	15	20	30	0087	5	40	10	20	20
0039	0	25	15	20	30	0088	0	25	20	20	30
0040	0	15	15	20	40	0089	0	25	20	20	30
0041	0	20	15	20	40	0090	10	30	20	20	30
0042	0	25	10	20	30	0091	10	25	20	20	30
0043	0	25	15	20	40	0092	0	15	20	20	30
0044	10	20	10	30	20	0093	0	30	10	30	10
0045	10	45	15	30	40	0094	5	30	20	30	20
0046	10	20	10	30	20	0095	0	40	20	10	20
0047	10	30	10	30	30	0096	10	25	20	20	10
0048	10	20	10	30	30	0097	0	30	20	20	20
0049	10	35	10	30	20	0098	10	45	20	20	20

APPENDIX 1 (cont.)

Sample XBS	Co	Cu	Ni	Pb	Zn	Sample XBS	Co	Cu	Ni	Pb	Zn
0099	10	30	30	10	20	0149	10	35	15	30	50
0100	10	30	40	10	20	0150	10	30	15	30	50
0101	10	70	20	10	50	0151	10	75	20	30	50
0102	10	50	20	10	20	0152	10	40	20	20	40
0103	10	45	40	10	20	0153	5	45	15	20	40
0104	10	50	30	10	40	0154	10	60	25	30	60
0105	40	50	20	10	30	0155	10	50	20	30	50
0106	10	10	20	20	20	0156	5	35	15	30	40
0107	10	20	20	20	50	0157	10	35	15	20	30
0108	10	20	20	20	40	0158	10	40	20	30	40
0109	10	25	10	20	50	0159	15	45	25	40	70
0110	10	20	10	30	40	0160	25	45	30	30	70
0111	10	30	20	30	50	0161	20	50	35	30	80
0112	10	30	20	20	50	0162	30	50	40	20	90
0113	10	40	20	20	60	0163	25	50	35	30	90
0114	10	20	10	20	50	0164	20	50	35	30	80
0115	10	20	20	20	40	0165	20	45	30	30	80
0116	10	30	20	20	50	0166	15	45	30	30	70
0117	10	30	20	20	50	0167	15	40	30	30	80
0118	10	25	10	20	40	0168	10	40	15	50	60
0119	10	25	10	20	40	0169	10	90	15	40	60
0120	10	25	20	10	20	0170	10	50	15	50	60
0121	10	20	20	10	30	0171	10	50	20	40	60
0122	15	20	20	20	40	0172	10	45	20	30	70
0123	10	30	40	10	20	0173	10	40	15	40	80
0124	10	20	20	40	20	0174	10	40	20	30	50
0125	10	20	20	20	20	0175	10	40	15	30	50
0126	10	40	20	20	20	0176	10	35	20	30	60
0127	10	20	20	20	10	0177	10	35	20	30	50
0128	0	20	20	10	20	0178	10	40	20	30	50
0129	10	30	20	20	20	0179	5	45	10	20	20
0130	10	30	20	20	20	0180	10	55	15	20	30
0131	10	40	20	20	40	0181	10	60	15	20	40
0132	10	50	25	20	40	0182	10	75	15	20	30
0133	5	40	15	20	30	0183	10	50	15	20	20
0134	5	25	15	20	30	0184	10	55	15	20	30
0135	15	40	35	20	60	0185	10	55	15	20	30
0136	20	45	15	20	30	0186	10	45	20	20	30
0137	5	30	10	30	40	0187	15	45	25	20	40
0138	10	35	15	30	60	0188	10	40	20	30	40
0139	10	30	15	30	50	0189	15	40	25	20	40
0140	10	35	20	30	50	0190	35	60	35	110	80
0141	10	35	15	30	60	0191	20	55	35	40	90
0142	10	50	15	90	90	0192	25	60	35	40	100
0143	10	40	15	50	70	0193	25	50	30	30	90
0144	10	35	15	30	50	0194	20	60	40	30	90
0145	10	40	15	40	60	0195	20	90	40	30	90
0146	10	35	15	30	50	0196	20	50	40	30	90
0147	10	40	15	30	60	0197	20	45	35	30	90
0148	10	40	15	30	60	0198	20	45	30	30	90

APPENDIX 1 (cont.)

Sample XBS	Co	Cu	Ni	Pb	Zn	Sample XBS	Co	Cu	Ni	Pb	Zn
0199	15	50	35	30	90	0220	10	45	10	40	80
0200	20	45	35	40	100	0221	10	50	20	40	90
0201	15	30	30	30	70	0222	10	20	15	30	30
0202	15	40	30	70	90	0223	5	0	20	30	20
0203	15	50	25	30	70	0224	10	20	20	30	40
0204	10	40	20	30	70	0225	10	20	25	30	30
0205	15	50	20	40	80	0226	10	30	20	20	30
0206	15	50	25	30	80	0227	10	20	25	20	30
0207	15	50	25	50	80	0228	10	30	10	30	20
0208	15	45	25	70	70	0229	10	25	15	20	40
0209	20	55	30	30	80	0230	10	40	20	20	20
0210	20	45	35	30	90	0231	10	45	20	10	30
0211	25	50	35	30	90	0232	10	30	20	30	50
0212	25	55	40	40	110	0233	5	40	20	30	30
0213	25	55	45	30	110	0234	10	50	30	20	40
0214	25	50	35	40	100	0235	10	35	30	30	60
0215	25	55	40	40	120	0236	10	40	10	30	40
0216	20	45	40	30	110	0237	15	50	10	40	90
0217	20	50	40	40	110	0238	15	40	10	30	50
0218	10	45	15	40	100	0239	15	45	10	20	30
0219	10	50	15	50	110	0240	10	90	10	30	80

APPENDIX 2 Soil analyses, OES.

In ppm except where otherwise stated

Sample XBS	B	Ba	Be	Cr	Fe%	Mn	Mo	Nb	Sn	V	Y	Zr
0001	1850	192	3.1	26	1.42	79	6.5	52	336	33	17.0	497
0002	2110	230	4.2	19	2.10	160	3.9	43	464	43	18.9	410
0003	1760	223	2.8	35	2.07	78	3.9	43	355	57	24.8	524
0004	1780	253	3.0	48	1.93	72	4.0	39	233	80	26.0	448
0005	1230	298	2.6	61	3.12	61	1.2	27	211	101	20.9	479
0006	1600	298	2.0	72	1.97	0	6.7	28	225	98	24.7	515
0007	1610	225	1.7	61	1.69	92	2.3	29	233	63	28.8	616
0008	946	210	1.6	96	3.77	97	1.2	0	35.1	136	27.5	468
0009	999	325	2.0	107	3.57	141	3.4	0	44.8	125	28.4	469
0010	783	294	1.6	93	4.28	112	0	28	39.2	113	20.9	440
0011	956	486	2.5	129	3.31	64	0	21	128	182	31.0	379
0012	793	236	1.6	109	3.26	95	1.5	26	41.5	117	22.1	477
0013	1040	255	1.8	103	2.95	111	3.3	0	285	125	23.9	489
0014	0	0	0	244	5.86	958	0	0	0	235	5.3	0
0015	758	295	1.6	91	4.23	55	0	22	181	132	23.5	435
0016	888	358	2.0	81	4.23	63	2.2	20	66.7	135	21.6	467
0017	1040	260	1.9	75	3.05	147	1.9	22	283	116	31.0	468
0018	900	320	1.9	107	3.66	0	1.0	0	57.1	137	23.2	430
0019	954	356	1.8	95	3.07	0	2.1	21	83.0	132	23.2	516
0020	1000	300	2.1	89	4.00	55	2.4	21	78.9	138	21.3	497
0021	1090	342	2.6	128	3.13	0	2.4	29	71.1	121	27.0	449
0022	901	303	1.9	98	3.09	0	5.7	29	44.6	131	26.9	628
0023	860	286	2.0	126	3.68	50	3.2	27	44.9	124	21.6	427
0024	1030	396	2.1	119	3.49	50	1.0	30	99.2	136	27.5	511
0025	1070	303	1.8	115	5.70	0	0	0	44.8	134	21.8	313
0026	1070	320	2.7	113	3.98	52	2.0	25	50.6	125	25.5	359
0027	797	403	2.8	130	3.19	64	2.5	24	53.6	146	35.2	545
0028	791	238	2.2	121	3.41	0	2.9	29	46.3	137	30.4	525
0029	942	244	1.8	147	3.73	154	1.8	20	67.1	139	26.6	441
0030	1040	278	1.7	121	3.95	130	2.2	21	55.8	134	24.1	423
0031	910	262	1.7	115	3.79	178	1.9	23	59.8	134	26.6	411
0032	854	344	1.8	137	3.85	101	1.0	25	32.2	143	28.4	520
0033	747	318	1.6	117	3.91	77	2.4	28	37.4	136	24.2	640
0034	788	333	1.8	107	3.38	82	2.0	26	51.8	126	26.2	491
0035	685	267	1.4	112	3.67	103	7.3	28	54.2	112	32.8	508
0036	766	427	1.9	149	4.02	112	3.2	0	42.4	119	38.7	629
0037	1170	301	2.1	115	4.21	80	1.7	24	68.1	127	23.0	354
0038	948	186	1.9	127	4.42	101	0	20	56.6	127	26.1	360
0039	1240	295	2.1	123	3.34	102	1.7	29	53.4	146	24.9	442
0040	762	292	1.5	105	3.48	62	2.4	26	38.0	112	24.0	577
0041	1100	291	1.9	99	3.73	82	1.5	32	46.7	117	27.2	476
0042	997	248	1.5	112	4.10	0	2.4	27	48.2	128	26.1	367
0043	1010	218	2.4	63	2.60	73	4.0	0	48.3	116	23.4	355
0044	818	286	3.2	65	3.72	0	1.3	24	41.4	106	18.3	377
0045	1660	353	3.8	98	4.62	72	1.4	0	99.7	113	25.1	309
0046	1010	309	1.9	86	2.75	0	3.4	20	69.6	104	23.8	381
0047	1080	359	2.3	76	2.54	0	3.5	0	94.8	140	31.8	294
0048	921	396	1.9	83	3.50	0	2.1	0	138	107	24.5	413
0049	717	466	3.0	95	2.29	0	7.0	0	94.7	150	27.7	269

APPENDIX 2 (cont.)

Sample XBS	B	Ba	Be	Cr	Fe%	Mn	Mo	Nb	Sn	V	Y	Zr
0050	1000	382	2.0	91	2.77	0	2.2	22	90.2	124	29.8	392
0051	1010	371	2.6	87	2.39	0	2.0	20	126	124	28.1	360
0052	654	347	1.8	99	4.44	87	8.4	22	54.6	116	24.1	382
0053	948	350	1.9	71	3.30	55	1.9	21	43.2	107	24.5	436
0054	703	317	1.6	82	3.38	0	14.8	21	59.1	116	25.8	389
0055	618	330	1.9	103	3.65	87	22.2	21	55.5	148	24.6	516
0056	1060	414	1.8	80	3.80	63	6.4	20	46.8	120	23.1	422
0057	1070	439	1.6	109	3.19	81	24.6	25	116	116	26.3	472
0058	1150	396	1.9	98	3.31	0	3.7	0	55.8	146	23.2	358
0059	1050	298	1.4	81	2.86	61	3.8	23	43.9	113	23.1	520
0060	751	439	1.4	95	2.56	73	3.6	20	52.0	151	29.6	493
0061	911	414	1.9	97	4.57	0	2.0	0	43.9	158	23.7	453
0062	699	370	1.8	85	2.42	0	6.5	25	44.9	123	24.0	342
0063	960	352	1.8	69	4.11	56	4.6	0	53.9	113	26.4	433
0064	915	411	2.0	108	4.67	65	2.5	0	42.6	123	26.0	405
0065	930	319	2.8	92	3.75	0	1.0	21	61.1	123	29.2	382
0066	1080	317	2.8	101	4.17	59	1.7	21	42.4	135	24.2	381
0067	1600	259	3.9	86	3.77	69	2.9	23	196	112	23.8	317
0068	1050	308	2.9	85	2.61	0	0	0	58.3	119	27.1	435
0069	1010	332	2.8	116	3.17	0	2.1	0	38.1	152	34.5	403
0070	739	345	3.0	127	2.16	53	2.8	0	55.1	176	41.5	381
0071	543	337	2.3	113	2.65	0	1.8	20	60.2	141	28.9	376
0072	968	317	2.0	82	3.17	69	1.3	23	89.1	116	26.6	402
0073	893	386	2.5	101	3.18	0	2.3	21	104	146	28.6	404
0074	617	273	2.0	107	3.15	83	4.1	20	78.8	140	25.2	363
0075	856	312	2.0	104	3.80	0	4.6	23	72.0	150	25.8	391
0076	896	372	2.5	103	3.70	62	5.4	0	93.0	162	21.4	385
0077	807	357	2.2	108	3.91	175	3.7	24	88.0	146	25.2	386
0078	1010	340	1.9	94	3.81	223	2.5	20	106	137	25.2	367
0079	915	291	2.3	92	3.66	262	1.7	21	166	116	26.5	364
0080	873	339	1.9	80	3.67	243	1.8	0	232	117	23.1	419
0081	1000	349	2.4	93	3.88	304	4.6	30	155	131	27.6	518
0082	967	287	2.3	98	3.89	282	3.9	22	176	113	27.3	408
0083	1020	266	2.1	105	4.01	267	4.0	20	166	125	24.5	379
0084	1280	365	2.1	91	3.54	184	3.3	22	123	132	24.9	411
0085	1260	310	2.4	125	3.19	173	2.9	23	97.1	126	25.5	368
0086	1030	411	2.7	106	3.51	123	1.1	22	92.2	131	27.6	321
0087	964	283	3.0	98	3.52	97	5.7	0	127	111	28.0	341
0088	841	352	2.0	114	3.82	106	2.6	25	100	112	25.4	361
0089	876	357	1.6	119	4.04	81	3.7	0	75.8	157	22.2	440
0090	661	392	2.0	121	4.57	0	2.6	21	59.1	140	24.3	343
0091	1060	265	1.9	105	3.90	73	1.8	0	59.5	117	18.4	295
0092	931	282	2.1	98	2.60	77	3.4	0	157	122	24.6	494
0093	1050	297	2.2	125	2.18	83	6.3	21	102	143	22.1	382
0094	681	335	2.0	109	2.26	61	5.0	20	121	147	27.2	425
0095	796	254	1.9	88	2.52	0	6.1	21	78.3	112	19.9	376
0096	1000	335	1.8	117	4.02	105	4.4	21	116	140	23.1	413
0097	890	300	2.4	109	3.62	113	2.1	21	156	125	22.1	389
0098	548	258	2.2	111	3.50	143	3.4	20	52.0	104	17.7	521
0099	571	335	2.6	90	3.65	53	0	20	86.1	123	23.5	494
0100	585	311	2.5	113	3.98	146	2.1	0	48.4	114	19.4	387

APPENDIX 2 (cont.)

Sample XBS	B	Ba	Be	Cr	Fe%	Mn	Mo	Nb	Sn	V	Y	Zr
0101	800	314	2.7	160	4.52	243	2.9	0	60.0	103	24.3	399
0102	1090	397	2.8	102	4.08	159	0	20	103	131	25.5	453
0103	1220	423	4.1	120	3.09	74	3.0	0	124	142	24.6	469
0104	540	357	2.3	125	3.96	153	2.9	0	66.4	139	22.3	385
0105	1090	315	4.1	101	4.06	149	2.7	21	95.7	123	22.7	358
0106	1320	273	2.4	106	3.40	220	1.2	20	147	108	20.0	423
0107	1160	320	2.0	112	3.67	293	1.0	0	145	106	23.9	399
0108	1220	352	2.8	115	4.17	280	0	0	155	131	25.1	460
0109	979	312	2.3	82	3.52	333	0	20	161	135	20.9	314
0110	956	255	2.3	73	3.36	326	1.6	0	174	122	24.9	398
0111	962	460	2.3	70	3.30	391	1.0	22	146	117	27.8	455
0112	894	317	2.4	70	3.41	304	0	21	168	139	29.0	446
0113	830	326	2.2	98	3.26	381	2.6	0	144	194	21.1	412
0114	1310	371	2.8	112	4.15	543	1.2	0	245	156	26.8	449
0115	1070	296	2.7	98	3.94	553	0	0	120	152	34.4	343
0116	865	293	2.4	92	3.51	405	1.0	0	185	147	25.7	356
0117	829	304	2.3	70	3.00	388	1.3	0	104	108	21.3	346
0118	1720	325	2.8	71	3.10	576	1.3	0	251	123	27.0	378
0119	1100	331	2.6	88	3.07	185	2.4	0	185	118	25.2	377
0120	1010	391	2.2	91	3.83	155	2.7	0	70.5	148	22.6	446
0121	983	320	2.3	75	3.15	172	0	21	91.2	130	23.4	412
0122	1110	359	2.4	87	2.88	213	1.7	20	158	128	26.3	402
0123	720	295	1.8	90	2.80	0	1.5	0	232	138	20.2	387
0124	1440	393	3.1	96	2.58	54	2.0	20	132	127	27.5	408
0125	968	361	2.5	87	2.96	109	1.3	0	98.9	116	23.5	422
0126	1340	314	3.6	105	3.34	105	1.0	0	153	123	30.6	374
0127	974	352	2.6	137	2.60	59	1.0	21	199	136	28.5	391
0128	612	264	2.1	109	3.79	87	3.4	20	53.0	129	22.9	432
0129	568	296	2.4	112	4.81	101	1.5	0	68.6	154	21.6	388
0130	660	394	2.7	95	4.48	108	1.9	0	90.3	139	22.0	424
0131	465	382	2.8	99	5.28	117	1.2	0	52.5	144	23.0	353
0132	546	393	2.7	80	4.79	117	1.9	24	59.9	133	19.6	412
0133	717	304	3.2	95	4.26	120	1.5	20	63.7	114	25.4	470
0134	978	342	3.2	93	4.53	132	1.2	21	208	116	25.9	497
0135	507	361	2.9	99	3.24	58	1.6	21	169	127	29.3	427
0136	294	354	2.6	106	3.59	584	1.9	20	56.9	138	29.7	401
0137	783	319	3.2	83	3.00	246	2.0	21	166	114	26.7	365
0138	1030	330	2.8	96	3.67	660	5.4	21	212	127	29.4	435
0139	929	320	2.3	89	3.16	499	1.6	24	190	97	23.1	390
0140	970	348	2.3	95	3.49	458	3.0	20	265	120	25.7	356
0141	874	338	2.5	112	3.49	447	2.0	20	199	126	23.9	397
0142	989	295	2.1	97	3.59	506	4.0	25	181	103	23.1	402
0143	908	351	2.2	108	3.73	703	4.3	0	274	127	25.6	387
0144	867	382	1.9	85	3.52	595	2.2	23	308	127	27.5	427
0145	1140	327	2.2	89	3.45	852	3.5	26	320	118	28.3	380
0146	1080	382	2.9	104	3.61	497	2.4	22	517	130	34.2	407
0147	765	286	1.8	89	3.32	398	5.5	21	139	115	29.1	433
0148	837	336	2.2	104	3.50	438	4.5	23	193	128	29.8	353
0149	819	297	3.0	90	3.53	401	2.3	0	151	121	27.1	321
0150	787	324	2.4	119	3.86	378	9.2	0	146	125	26.9	358
0151	791	345	1.8	94	3.44	265	7.2	24	76.9	127	25.0	363

APPENDIX 2 (cont.)

Sample XBS	B	Ba	Be	Cr	Fe%	Mn	Mo	Nb	Sn	V	Y	Zr
0152	1480	335	4.9	101	4.06	278	4.8	27	247	132	30.2	253
0153	548	399	2.4	99	3.87	106	1.1	0	63.2	115	22.1	287
0154	580	426	2.5	87	2.87	112	1.6	22	110	150	27.2	380
0155	501	520	3.3	130	5.41	131	0	25	96.8	166	28.3	358
0156	598	365	2.5	111	4.78	84	0	0	53.3	144	24.8	418
0157	646	437	2.7	105	4.07	78	2.3	23	91.8	108	23.6	548
0158	549	301	3.4	113	4.02	91	1.4	22	264	118	22.6	414
0159	522	369	2.8	97	3.77	596	1.8	24	208	132	20.7	326
0160	617	362	4.0	113	4.95	612	2.8	20	130	123	21.6	321
0161	357	441	2.7	128	4.27	622	0	23	87.5	143	22.1	357
0162	456	346	3.5	136	4.68	1140	0	21	130	146	25.2	367
0163	374	427	3.0	120	4.48	1070	1.1	20	321	128	25.9	372
0164	369	323	2.7	118	4.71	1040	0	20	95.2	121	31.2	468
0165	347	301	2.2	113	4.52	1120	0	22	188	126	23.8	358
0166	355	501	2.3	128	4.36	646	1.4	22	115	120	30.5	560
0167	382	327	2.6	130	4.31	1000	0	23	171	123	28.6	477
0168	1160	452	4.1	115	3.50	420	0	23	213	124	27.1	332
0169	1180	378	3.4	118	3.38	598	0	22	366	111	24.5	391
0170	1250	429	4.3	97	3.53	520	0	27	314	118	28.1	418
0171	998	255	2.9	125	3.62	458	0	24	311	110	24.8	353
0172	799	352	2.6	139	3.75	536	0	21	206	106	34.5	427
0173	1240	375	3.2	147	3.79	858	0	23	312	108	26.4	367
0174	1120	313	3.1	99	3.72	704	0	24	308	107	24.1	386
0175	1100	374	2.9	100	3.45	747	0	0	338	104	31.1	362
0176	1020	267	2.7	72	3.16	647	0	0	302	104	22.1	318
0177	776	352	2.1	80	3.29	328	1.5	23	201	110	20.5	395
0178	960	306	3.0	89	4.19	251	0	0	190	115	21.5	286
0179	173	594	2.5	144	2.89	0	0	21	36.9	180	24.2	241
0180	1820	383	4.6	106	3.69	0	0	0	301	133	22.0	239
0181	1900	351	4.5	104	5.06	56	1.4	0	414	131	26.8	294
0182	2300	388	6.0	109	5.41	0	1.3	0	501	120	27.1	340
0183	689	388	3.9	121	3.25	52	0	22	43.4	126	33.1	432
0184	737	408	3.5	117	3.87	0	0	20	131	122	25.2	330
0185	709	380	3.8	120	4.92	53	0	20	71.7	146	29.8	368
0186	673	308	3.5	92	3.64	55	0	0	67.1	105	23.7	352
0187	688	408	3.8	122	4.09	102	1.5	0	316	117	28.0	418
0188	801	432	9.0	136	4.69	148	1.8	20	111	133	29.5	428
0189	705	304	3.5	110	3.60	204	1.3	21	230	122	25.0	379
0190	963	410	5.0	111	4.25	1290	1.1	24	307	127	29.7	348
0191	342	308	4.0	133	3.93	998	0	0	100	125	23.9	261
0192	390	386	3.1	118	4.00	1160	0	0	110	138	27.3	367
0193	403	502	3.6	121	4.02	1400	1.5	20	258	127	29.7	408
0194	465	502	4.1	149	4.74	763	0	21	85.3	150	28.5	322
0195	343	389	3.7	123	4.81	845	1.3	21	81.6	134	24.6	320
0196	362	387	3.0	138	4.61	985	0	0	85.1	131	23.7	337
0197	357	377	2.4	73	3.61	749	8.2	20	124	101	21.2	293
0198	277	260	1.7	84	3.32	701	0	0	89.4	92	19.0	450
0199	320	332	2.1	78	3.86	702	5.6	0	252	107	23.3	299
0200	334	402	1.9	145	4.24	756	1.9	0	159	115	29.5	368
0201	238	305	1.5	81	3.83	556	0	23	171	114	21.2	504
0202	354	334	2.0	78	3.71	767	1.9	20	157	117	28.2	376

APPENDIX 2 (cont.)

Sample XBS	B	Ba	Be	Cr	Fe%	Mn	Mo	Nb	Sn	V	Y	Zr
0203	467	333	2.7	79	3.63	246	2.1	25	181	119	23.1	376
0204	501	313	2.7	69	3.15	284	1.3	0	257	108	24.7	342
0205	431	373	2.4	69	3.46	396	2.5	0	382	116	30.5	370
0206	466	308	2.6	73	3.60	559	2.0	0	271	111	24.8	355
0207	336	320	2.1	85	3.59	587	1.6	0	305	126	26.3	341
0208	339	297	2.1	99	3.34	563	1.5	0	159	121	21.8	410
0209	368	321	2.5	88	4.30	945	0	0	261	127	23.5	375
0210	298	358	2.3	92	4.01	885	0	0	146	120	23.6	312
0211	265	286	2.0	71	3.96	1080	1.0	0	230	120	20.4	345
0212	368	377	2.8	86	4.52	998	0	0	175	140	25.8	297
0213	343	328	2.5	116	4.45	1080	1.0	0	206	125	25.3	243
0214	317	394	3.2	89	4.08	1020	0	0	166	134	28.0	312
0215	343	399	2.7	94	4.31	1070	0	0	174	138	27.9	292
0216	284	344	1.9	97	4.67	968	1.1	0	90.6	122	24.1	334
0217	359	358	2.5	97	4.29	1140	0	0	233	128	23.7	401
0218	305	320	2.2	87	4.59	709	0	0	26.0	126	25.3	339
0219	202	271	1.7	104	3.92	1050	1.6	0	141	116	20.3	342
0220	333	178	2.0	100	3.56	884	3.4	0	175	146	20.5	562
0221	206	296	1.4	87	3.02	801	0	20	88.6	144	19.7	470
0222	850	328	2.4	130	2.94	117	2.1	0	37.2	178	26.4	533
0223	1530	173	1.9	82	1.71	61	1.5	24	407	94	28.3	555
0224	872	290	1.8	108	3.05	162	2.7	0	56.1	152	19.4	366
0225	820	332	1.7	119	2.85	96	3.9	0	36.1	152	24.1	522
0226	1140	334	2.9	106	3.32	81	3.2	23	113	184	23.5	571
0227	1150	335	1.4	95	2.85	199	1.7	20	50.7	138	18.0	440
0228	1230	349	1.9	124	2.50	179	1.4	0	176	172	23.4	435
0229	690	247	1.0	86	2.59	163	1.2	20	82.6	133	18.6	512
0230	454	301	1.5	123	2.59	198	1.8	23	72.8	146	32.6	660
0231	993	470	3.1	113	3.14	193	1.6	0	83.6	162	24.5	405
0232	1050	269	1.9	120	3.54	277	1.2	0	183	139	24.7	381
0233	1620	615	3.4	150	3.69	245	5.4	22	235	230	35.1	413
0234	399	289	1.4	92	3.33	252	2.1	0	53.5	113	18.3	498
0235	1080	372	2.2	141	3.04	572	7.2	23	235	171	26.8	511
0236	595	510	1.9	134	3.99	127	23.8	0	130	166	31.4	474
0237	306	381	2.1	174	4.99	1320	7.8	0	239	242	34.4	441
0238	663	386	1.7	97	3.69	194	16.5	0	124	162	22.5	391
0239	387	346	1.5	88	2.75	117	7.1	0	43.0	156	24.1	542
0240	249	362	2.1	124	3.41	535	4.7	0	42.7	181	23.5	377

APPENDIX 3 Soil analyses, XRF.

In ppm except where otherwise stated

Sample XBS	Ba	Ca%	Ce	Fe%	Mn	Sb	Sn	Ti%	W
0001	183	0.130	54	2.474	170	7	354	0.452	162*
0002	193	0.062	63	3.408	220	9	341	0.416	81*
0003	235	0.086	52	3.321	160	5	255	0.564	166*
0004	264	0.094	55	3.718	140	4	203	0.641	131*
0005	293	0.084	52	4.732	120	0	151	0.674	128*
0006	245	0.138	58	3.291	110	7	224	0.659	151*
0007	183	0.081	39	2.833	120	3	184	0.645	219*
0008	377	0.225	51	5.638	170	11	53	0.726	79*
0009	371	0.177	42	5.299	240	2	46	0.700	13
0010	326	0.260	61	6.358	220	9	48	0.692	12
0011	447	0.137	63	4.491	150	12	129	0.762	14
0012	351	0.248	66	4.993	180	10	62	0.735	9
0013	393	0.232	55	5.694	170	4	89	0.684	18
0014	351	0.244	67	5.966	170	5	87	0.682	15
0015	339	0.266	54	5.929	130	4	134	0.721	15
0016	359	0.217	50	5.885	150	12	89	0.682	14
0017	305	0.319	53	4.752	210	4	257	0.717	17
0018	379	0.126	64	5.054	120	6	61	0.700	12
0019	355	0.202	59	4.571	110	4	88	0.747	12
0020	378	0.253	60	5.791	130	1	102	0.726	11
0021	390	0.175	37	4.882	90	5	91	0.751	8
0022	369	0.078	59	4.886	90	10	71	0.732	10
0023	397	0.151	45	5.206	90	5	55	0.721	12
0024	390	0.175	90	5.052	80	7	76	0.754	17
0025	364	0.267	52	7.587	90	11	82	0.719	17
0026	403	0.145	72	5.571	90	3	70	0.748	14
0027	424	0.160	82	4.890	90	6	55	0.734	12
0028	410	0.173	75	5.115	100	2	65	0.731	13
0029	331	0.180	69	5.306	230	0	82	0.691	13
0030	344	0.141	80	5.577	190	7	77	0.731	17
0031	350	0.119	69	5.367	230	0	72	0.724	14
0032	398	0.170	74	5.085	170	7	48	0.714	11
0033	339	0.156	48	5.169	150	5	39	0.719	11
0034	418	0.147	78	5.007	150	4	60	0.724	12
0035	364	0.140	62	5.694	180	2	54	0.696	10
0036	351	0.276	44	5.457	180	3	53	0.680	9
0037	376	0.164	53	5.888	150	1	74	0.725	12
0038	379	0.191	66	6.506	140	0	62	0.708	11
0039	415	0.154	71	5.050	120	7	59	0.780	14
0040	355	0.125	58	5.166	150	5	56	0.715	10
0041	366	0.157	46	5.391	110	0	82	0.742	12
0042	391	0.146	41	6.040	110	7	58	0.746	12
0043	398	0.151	51	4.913	100	0	46	0.737	11
0044	367	0.194	58	5.760	100	7	57	0.728	11
0045	380	0.190	107	6.631	150	12	147	0.707	26
0046	333	0.213	62	4.418	100	0	105	0.765	16
0047	388	0.134	60	3.862	110	7	133	0.742	17
0048	354	0.207	54	5.384	120	8	78	0.723	15
0049	441	0.140	71	3.435	70	8	91	0.731	13

APPENDIX 3 (cont.)

Sample XBS	Ba	Ca%	Ce	Fe%	Mn	Sb	Sn	Ti%	W
0050	367	0.181	72	4.274	90	5	101	0.769	13
0051	373	0.100	62	2.848	100	7	146	0.571	12
0052	344	0.144	57	6.215	180	2	45	0.699	10
0053	321	0.211	52	5.559	150	0	68	0.766	13
0054	355	0.135	69	5.254	160	5	53	0.817	10
0055	379	0.106	49	5.718	160	1	47	0.859	16
0056	398	0.166	77	5.967	170	5	92	0.728	15
0057	333	0.195	67	4.816	170	6	105	0.764	13
0058	392	0.164	51	5.086	100	5	64	0.733	12
0059	350	0.177	59	4.533	90	4	62	0.786	13
0060	370	0.143	61	4.139	90	5	58	0.764	12
0061	364	0.189	49	6.555	120	9	69	0.750	12
0062	427	0.113	48	4.438	70	0	68	0.787	12
0063	345	0.145	62	6.374	120	10	74	0.746	10
0064	370	0.120	47	6.601	110	2	62	0.725	13
0065	362	0.164	63	5.437	120	6	59	0.744	13
0066	392	0.123	39	5.960	100	4	66	0.850	13
0067	404	0.078	57	5.517	110	0	216	0.733	20
0068	401	0.102	79	4.218	80	8	89	0.765	15
0069	386	0.128	74	4.568	110	0	83	0.746	13
0070	493	0.066	109	3.426	80	3	50	0.802	6
0071	404	0.107	49	4.173	90	16	101	0.732	10
0072	332	0.157	58	4.823	80	9	113	0.759	13
0073	347	0.094	69	4.776	80	3	100	0.763	12
0074	418	0.078	47	4.868	70	6	90	0.764	9
0075	403	0.084	72	5.783	100	3	123	0.756	11
0076	447	0.089	55	5.598	80	1	131	0.793	13
0077	386	0.122	62	5.563	250	5	104	0.736	14
0078	338	0.167	65	5.509	320	5	153	0.731	14
0079	334	0.218	49	5.221	340	5	175	0.714	14
0080	361	0.170	63	5.435	340	11	156	0.730	12
0081	365	0.206	55	5.590	350	6	187	0.713	13
0082	365	0.173	81	5.663	350	2	164	0.710	12
0083	367	0.214	76	5.587	370	8	167	0.756	14
0084	360	0.176	58	5.061	270	0	165	0.762	13
0085	354	0.130	64	4.836	240	4	158	0.747	14
0086	414	0.147	68	5.179	210	7	103	0.740	10
0087	357	0.058	75	5.350	110	9	103	0.745	14
0088	382	0.103	53	5.660	120	5	76	0.744	11
0089	395	0.130	55	5.791	100	6	79	0.776	11
0090	422	0.096	62	6.204	90	9	68	0.738	9
0091	375	0.170	61	6.254	110	13	111	0.758	14
0092	328	0.048	62	4.174	100	5	131	0.788	11
0093	357	0.045	76	3.730	70	4	107	0.777	10
0094	325	0.061	60	3.831	60	2	117	0.744	7
0095	365	0.112	83	4.564	100	8	106	0.779	14
0096	337	0.181	73	5.753	90	3	98	0.749	11
0097	386	0.190	43	5.617	100	3	164	0.784	14
0098	385	0.175	50	5.606	110	9	87	0.764	12
0099	396	0.177	41	5.422	130	3	95	0.790	14

APPENDIX 3 (cont.)

Sample XBS	Ba	Ca%	Ce	Fe%	Mn	Sb	Sn	Ti%	W
0100	455	0.187	49	5.975	110	3	73	0.703	13
0101	462	0.226	63	5.829	220	0	76	0.753	9
0102	394	0.177	57	6.465	190	0	86	0.653	12
0103	426	0.146	61	4.512	140	4	183	0.813	15
0104	451	0.160	71	6.267	100	3	125	0.772	13
0105	443	0.135	128	5.658	270	1	125	0.707	30
0106	343	0.140	65	5.075	320	6	178	0.750	21
0107	336	0.186	62	5.464	410	6	197	0.714	21
0108	342	0.143	77	5.971	370	0	154	0.710	17
0109	354	0.181	54	5.731	410	6	210	0.690	16
0110	360	0.133	80	5.534	410	6	180	0.710	15
0111	346	0.116	72	5.392	480	5	190	0.704	16
0112	336	0.173	82	5.148	440	5	192	0.705	15
0113	350	0.147	63	5.498	450	0	173	0.701	15
0114	339	0.162	61	5.594	500	3	196	0.697	15
0115	360	0.175	54	5.381	480	3	203	0.709	15
0116	381	0.162	56	5.634	490	10	178	0.712	14
0117	343	0.140	66	5.323	460	9	204	0.683	13
0118	328	0.165	61	5.487	540	4	203	0.738	16
0119	359	0.150	59	5.378	300	0	174	0.740	16
0120	396	0.124	45	6.079	200	2	117	0.746	16
0121	349	0.170	54	5.352	220	3	151	0.747	17
0122	311	0.142	87	4.675	280	5	185	0.717	17
0123	385	0.097	43	5.122	100	14	310	0.744	14
0124	345	0.210	60	4.043	110	4	128	0.787	15
0125	326	0.165	72	4.617	110	15	110	0.746	10
0126	346	0.042	62	5.148	100	6	186	0.722	13
0127	343	0.273	56	4.561	100	4	189	0.815	12
0128	389	0.271	62	6.153	130	0	81	0.800	11
0129	408	0.189	48	6.882	130	9	79	0.765	9
0130	438	0.203	56	7.152	130	7	101	0.776	7
0131	465	0.133	63	7.233	180	6	66	0.746	5
0132	431	0.201	57	6.802	200	1	68	0.726	8
0133	409	0.155	56	6.174	200	6	93	0.726	10
0134	362	0.224	59	6.046	140	3	189	0.781	11
0135	376	0.134	61	4.745	110	5	169	0.790	11
0136	429	0.102	81	5.340	630	0	47	0.719	5
0137	398	0.151	69	4.466	290	2	158	0.766	10
0138	354	0.106	62	5.144	600	11	213	0.686	16
0139	344	0.138	60	5.055	520	5	238	0.671	16
0140	359	0.119	59	5.068	470	6	220	0.686	15
0141	371	0.118	71	5.201	500	0	200	0.692	16
0142	332	0.109	69	4.922	510	5	219	0.646	16
0143	360	0.153	75	5.248	680	0	308	0.685	13
0144	370	0.073	60	5.117	630	8	264	0.697	13
0145	343	0.099	72	5.132	660	4	270	0.723	12
0146	322	0.145	61	5.362	480	0	470	0.690	13
0147	370	0.127	57	5.260	510	10	209	0.745	13
0148	352	0.132	60	5.272	510	4	230	0.725	15
0149	369	0.143	66	5.074	420	7	166	0.715	13

APPENDIX 3 (cont.)

Sample XBS	Ba	Ca%	Ce	Fe%	Mn	Sb	Sn	Ti%	W
0150	379	0.141	72	5.286	390	4	169	0.719	10
0151	370	0.184	41	5.003	380	1	174	0.720	11
0152	431	0.100	87	5.752	330	11	268	0.661	19
0153	392	0.061	46	5.502	160	12	99	0.752	5
0154	371	0.059	61	4.083	140	7	147	0.767	11
0155	432	0.098	66	6.760	180	2	83	0.727	8
0156	384	0.061	48	6.239	150	2	87	0.744	12
0157	357	0.108	52	5.833	160	2	111	0.763	11
0158	391	0.115	67	5.701	190	7	256	0.715	11
0159	367	0.119	59	5.401	580	13	181	0.704	13
0160	397	0.103	75	6.615	670	8	131	0.682	20
0161	446	0.099	74	5.789	640	5	108	0.687	7
0162	438	0.075	90	6.303	830	1	133	0.708	5
0163	373	0.185	82	6.310	880	0	372	0.678	8
0164	392	0.174	74	6.216	900	0	140	0.714	5
0165	395	0.178	74	6.207	1020	0	214	0.738	7
0166	401	0.138	73	5.502	620	3	130	0.731	6
0167	389	0.163	61	5.876	750	0	137	0.731	6
0168	397	0.136	80	4.632	450	9	248	0.710	14
0169	389	0.135	76	4.837	550	2	336	0.719	16
0170	371	0.117	64	4.882	510	11	279	0.706	16
0171	372	0.192	66	5.062	470	1	295	0.706	15
0172	381	0.282	63	5.006	510	6	204	0.683	15
0173	338	0.105	60	5.166	670	6	274	0.709	16
0174	349	0.074	63	5.177	590	11	309	0.691	12
0175	341	0.090	69	5.210	710	10	308	0.704	14
0176	356	0.100	60	5.132	630	5	267	0.724	15
0177	377	0.096	48	5.348	460	2	219	0.705	15
0178	337	0.072	47	6.090	350	0	209	0.665	13
0179	518	0.030	43	4.364	80	5	65	0.733	7
0180	409	0.048	90	5.396	120	8	413	0.729	17
0181	364	0.045	68	7.128	130	3	349	0.735	14
0182	340	0.048	62	7.825	110	0	453	0.714	12
0183	413	0.042	41	4.783	80	2	72	0.749	12
0184	379	0.043	53	5.564	80	10	126	0.722	10
0185	404	0.054	60	6.599	90	1	100	0.753	13
0186	373	0.057	50	5.668	100	1	94	0.739	17
0187	389	0.090	47	5.789	190	3	219	0.715	12
0188	430	0.165	72	6.035	180	2	135	0.751	11
0189	393	0.093	54	5.628	310	0	184	0.730	9
0190	385	0.078	82	5.847	970	11	214	0.731	11
0191	357	0.152	74	5.889	840	9	154	0.679	9
0192	377	0.119	68	5.879	950	7	184	0.697	8
0193	392	0.130	66	5.928	980	0	208	0.703	8
0194	483	0.152	73	6.469	720	6	123	0.730	7
0195	417	0.157	60	6.452	780	2	109	0.688	9
0196	405	0.192	68	6.320	860	1	110	0.701	7
0197	375	0.311	64	6.048	810	2	121	0.687	5
0198	334	0.212	69	5.748	830	2	114	0.687	4
0199	370	0.249	56	6.111	790	2	158	0.686	10

APPENDIX 3 (cont.)

Sample XBS	Ba	Ca%	Ce	Fe%	Mn	Sb	Sn	Ti%	W
0200	370	0.209	53	6.005	800	0	164	0.695	8
0201	392	0.136	70	6.151	720	5	136	0.685	4
0202	357	0.177	62	5.895	810	2	173	0.699	7
0203	363	0.092	40	5.591	380	8	200	0.723	13
0204	336	0.105	64	5.399	430	3	240	0.731	12
0205	348	0.106	41	5.498	530	3	333	0.726	12
0206	364	0.115	61	5.690	610	2	271	0.715	11
0207	360	0.114	74	5.487	710	8	263	0.710	11
0208	362	0.152	57	5.449	670	12	219	0.705	8
0209	371	0.126	63	6.210	1040	5	265	0.692	10
0210	402	0.110	71	5.972	910	2	171	0.708	9
0211	399	0.388	51	6.134	1270	7	267	0.711	7
0212	375	0.213	62	6.336	1010	0	206	0.696	11
0213	391	0.232	69	6.450	1080	8	189	0.681	10
0214	397	0.180	70	6.189	990	5	152	0.702	8
0215	385	0.170	50	6.531	990	4	184	0.689	8
0216	403	0.182	74	6.595	1050	0	124	0.702	6
0217	367	0.220	52	6.344	870	8	171	0.678	6
0218	395	0.183	63	6.679	930	0	144	0.699	7
0219	63	0.195	7	6.186	500	4	52	0.685	10
0220	364	0.114	57	5.692	970	2	307	0.702	10
0221	420	0.374	69	6.220	1150	2	183	0.707	9
0222	361	0.223	40	5.579	190	16	57	0.839	15
0223	203	0.099	44	3.373	120	3	461	0.605	14
0224	362	0.183	66	5.459	230	5	98	0.697	15
0225	360	0.204	52	5.960	140	8	61	0.695	8
0226	383	0.164	103	5.998	130	7	112	0.716	18
0227	337	0.188	62	5.141	190	3	101	0.766	17
0228	379	0.070	69	4.972	110	6	207	0.743	18
0229	365	0.157	58	5.839	350	10	145	0.726	17
0230	391	0.176	48	5.674	100	3	101	0.785	12
0231	431	0.102	151	5.468	220	6	105	0.707	32
0232	360	0.167	75	5.950	420	8	190	0.691	18
0233	350	0.035	81	5.281	110	8	173	0.710	16
0234	389	0.169	40	6.273	190	7	87	0.721	9
0235	337	0.114	69	5.409	580	3	227	0.645	17
0236	373	0.075	74	6.365	150	4	115	0.726	12
0237	369	0.184	52	6.492	1140	4	207	0.729	10
0238	357	0.057	44	5.995	340	5	201	0.657	13
0239	368	0.041	58	5.425	110	8	82	0.743	17
0240	417	0.146	68	6.510	830	7	90	0.682	12

* Sample ground in tungsten carbide Tema mill

APPENDIX 4 Soil analyses, loss on ignition

Sample XBS	LOI%	Sample XBS	LOI%	Sample XBS	LOI%	Sample XBS	LOI%	Sample XBS	LOI%
0001	15.1	0049	8.5	0097	7.6	0145	13.9	0193	8.2
0002	11.9	0050	9.4	0098	3.8	0146	5.5	0194	7.1
0003	12.8	0051	6.2	0099	5.0	0147	4.7	0195	6.6
0004	14.8	0052	11.1	0100	3.1	0148	5.4	0196	6.9
0005	11.3	0053	9.7	0101	6.5	0149	6.7	0197	5.7
0006	14.0	0054	7.8	0102	3.4	0150	4.3	0198	6.6
0007	11.9	0055	7.5	0103	5.3	0151	5.6	0199	5.9
0008	10.1	0056	15.7	0104	6.0	0152	7.5	0200	8.4
0009	11.6	0057	12.4	0105	2.6	0153	5.5	0201	6.4
0010	13.6	0058	10.6	0106	7.2	0154	11.3	0202	7.0
0011	8.4	0059	8.2	0107	6.9	0155	9.4	0203	6.5
0012	11.7	0060	8.9	0108	5.2	0156	6.6	0204	9.3
0013	8.0	0061	10.0	0109	7.5	0157	10.0	0205	9.0
0014	10.0	0062	5.7	0110	6.6	0158	9.1	0206	7.5
0015	10.1	0063	7.4	0111	6.3	0159	9.4	0207	6.8
0016	7.1	0064	7.4	0112	5.6	0160	4.7	0208	7.0
0017	9.4	0065	8.2	0113	8.6	0161	6.7	0209	6.1
0018	7.4	0066	9.5	0114	9.2	0162	8.6	0210	8.3
0019	6.5	0067	9.1	0115	11.1	0163	10.3	0211	7.6
0020	9.8	0068	4.8	0116	5.5	0164	8.8	0212	9.7
0021	8.8	0069	8.7	0117	6.2	0165	7.3	0213	8.5
0022	7.4	0070	4.1	0118	8.8	0166	7.0	0214	3.3
0023	10.2	0071	9.6	0119	9.1	0167	7.0	0215	11.5
0024	13.5	0072	8.6	0120	2.8	0168	9.0	0216	9.5
0025	10.7	0073	7.5	0121	4.4	0169	10.3	0217	9.6
0026	10.0	0074	2.7	0122	9.7	0170	9.3	0218	6.5
0027	10.2	0075	7.2	0123	3.1	0171	9.6	0219	11.0
0028	7.4	0076	3.7	0124	5.7	0172	5.7	0220	7.7
0029	9.5	0077	5.3	0125	8.6	0173	9.5	0221	6.0
0030	7.1	0078	6.3	0126	9.9	0174	8.8	0222	8.2
0031	7.6	0079	2.0	0127	10.5	0175	6.9	0223	11.4
0032	10.3	0080	5.6	0128	11.5	0176	4.0	0224	5.6
0033	9.8	0081	7.7	0129	6.2	0177	6.1	0225	6.5
0034	9.1	0082	6.9	0130	9.3	0178	10.3	0226	9.6
0035	12.3	0083	7.3	0131	6.7	0179	0.0	0227	8.3
0036	7.9	0084	4.8	0132	7.0	0180	6.6	0228	7.9
0037	10.0	0085	8.6	0133	5.3	0181	8.2	0229	4.2
0038	10.9	0086	4.9	0134	7.9	0182	6.1	0230	10.6
0039	7.0	0087	8.6	0135	4.6	0183	1.5	0231	2.7
0040	9.4	0088	7.7	0136	3.1	0184	4.8	0232	7.6
0041	12.1	0089	3.4	0137	6.7	0185	7.5	0233	11.5
0042	9.4	0090	6.8	0138	6.7	0186	5.9	0234	6.9
0043	6.6	0091	6.1	0139	5.0	0187	6.8	0235	6.1
0044	7.7	0092	5.9	0140	6.2	0188	7.4	0236	7.8
0045	8.2	0093	12.3	0141	4.1	0189	5.3	0237	5.4
0046	8.1	0094	15.1	0142	8.5	0190	9.3	0238	7.8
0047	7.8	0095	7.5	0143	8.3	0191	9.2	0239	2.5
0048	8.3	0096	8.5	0144	5.9	0192	7.5	0240	6.5

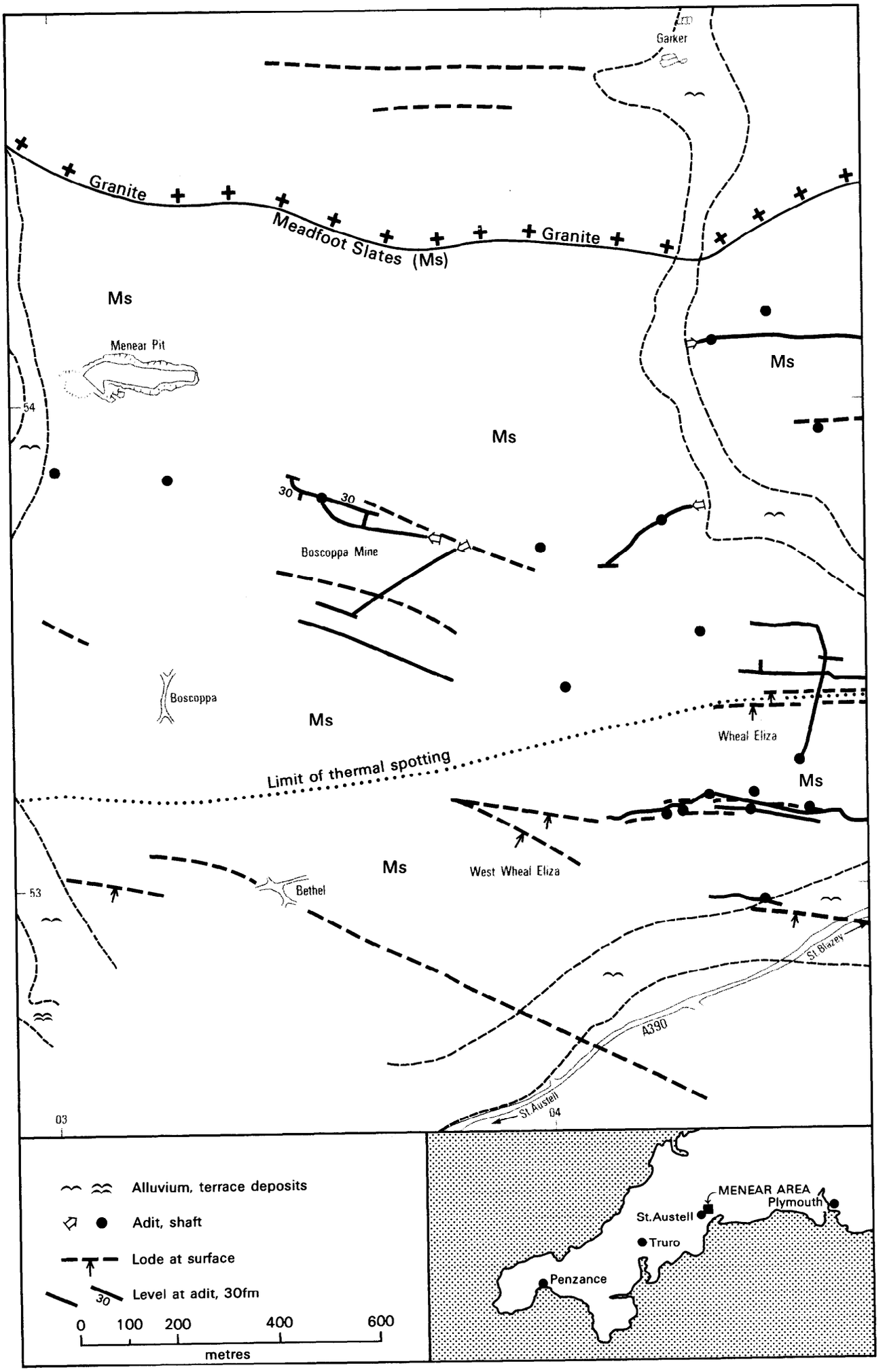

Figure 1 Geology and mining around Menear

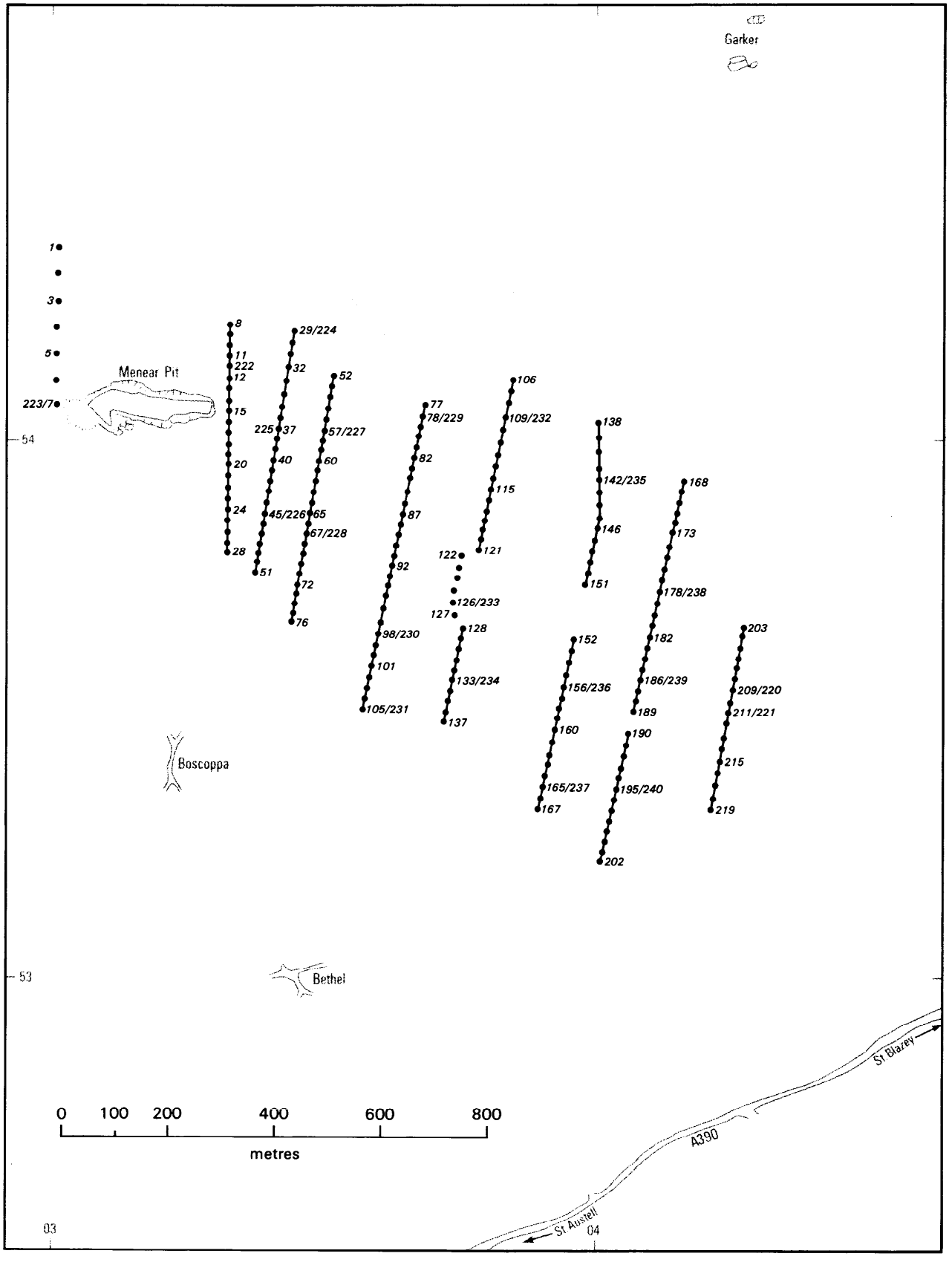

Figure 2 Soil sampling locations

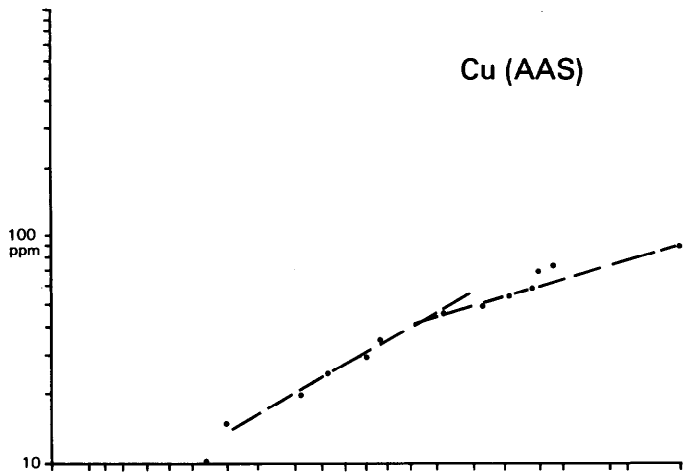

Figure 3 Log-probability plot for Cu (AAS)

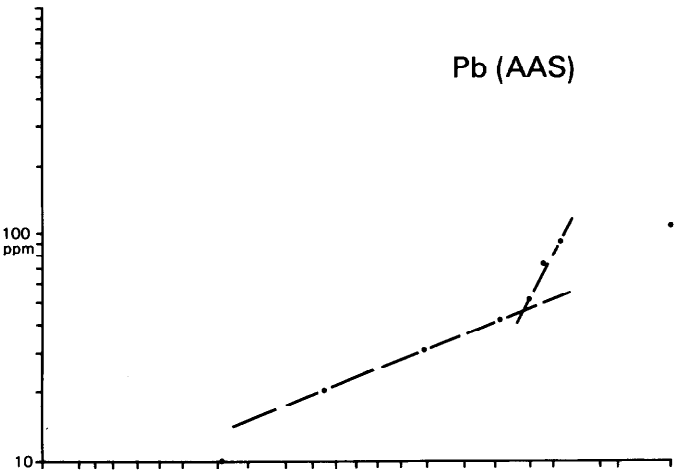

Figure 4 Log-probability plot for Pb (AAS)

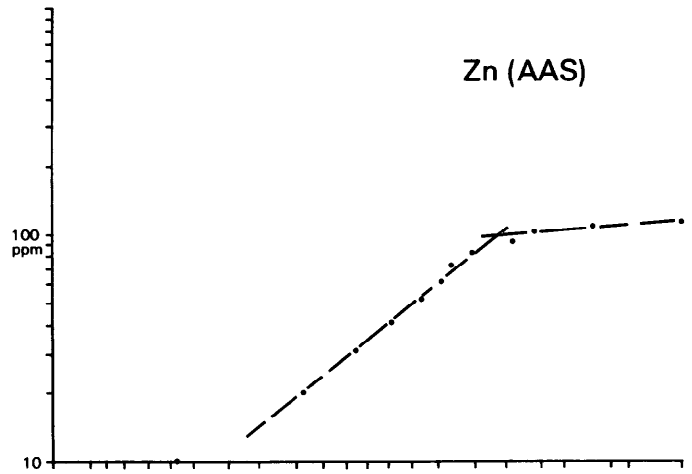

Figure 5 Log-probability plot for Zn (AAS)

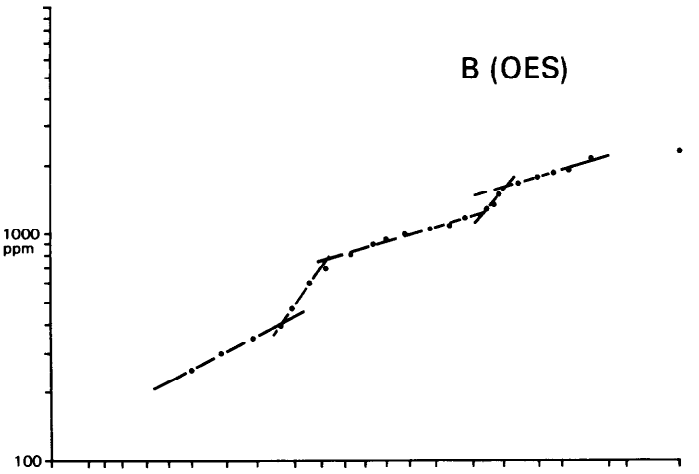

Figure 6 Log-probability plot for B (OES)

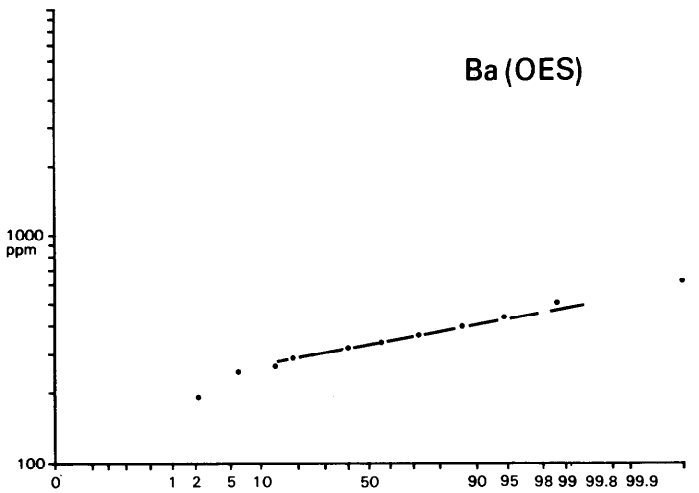

Figure 7 Log-probability plot for Ba (OES)

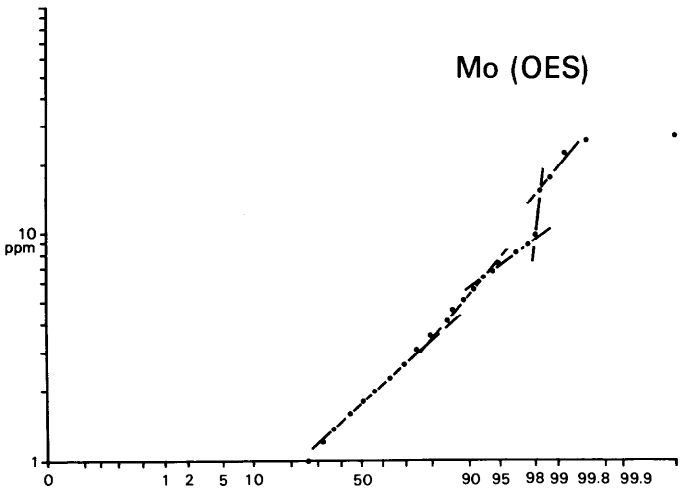

Figure 8 Log-probability plot for Mo (OES)

Log-probability plots

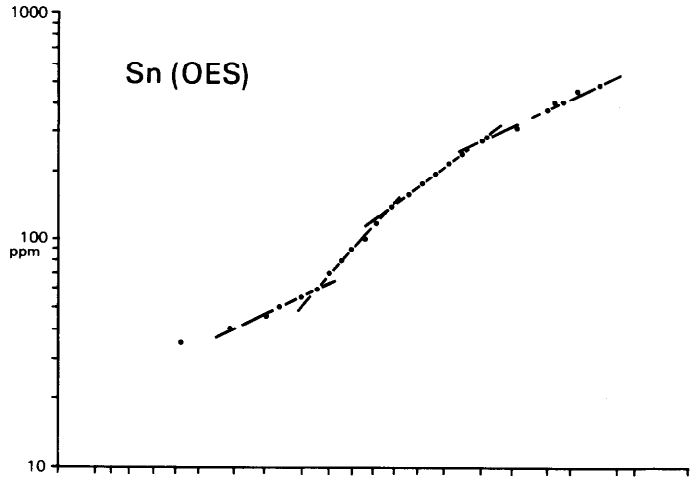

Figure 9 Log-probability plot for Sn (OES)

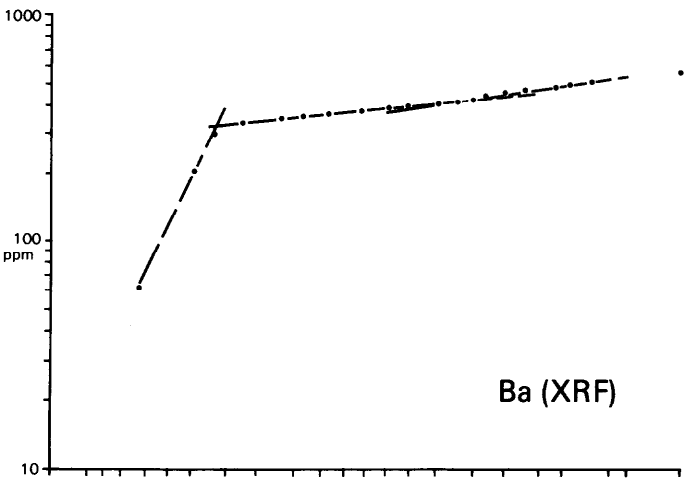

Figure 10 Log-probability plot for Ba (XRF)

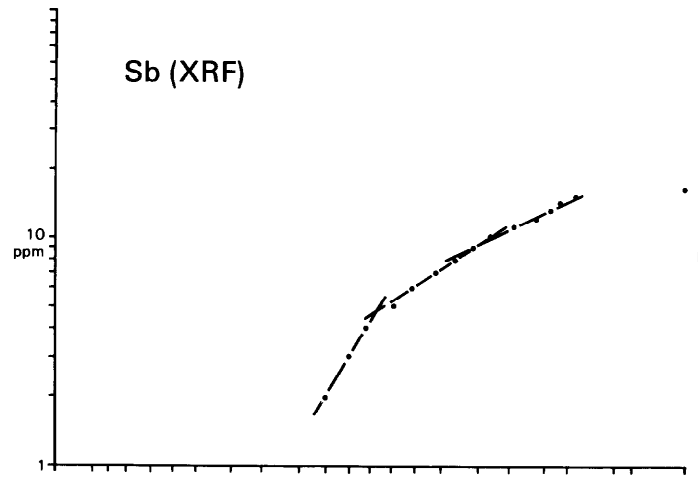

Figure 11 Log-probability plot for Sb (XRF)

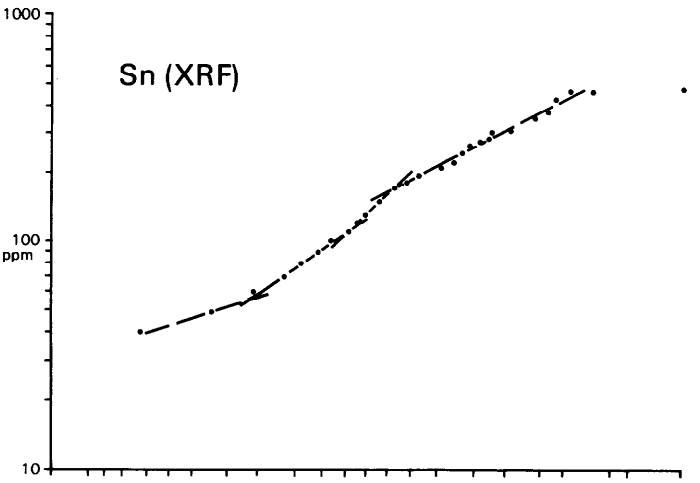

Figure 12 Log-probability plot for Sn (XRF)

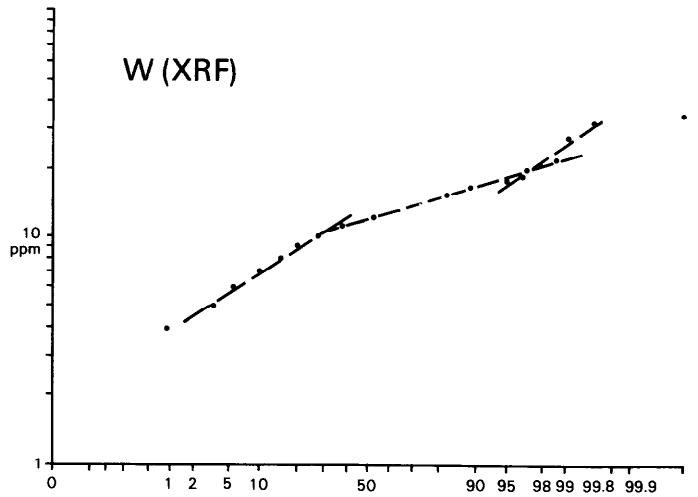

Figure 13 Log-probability plot for W (XRF)

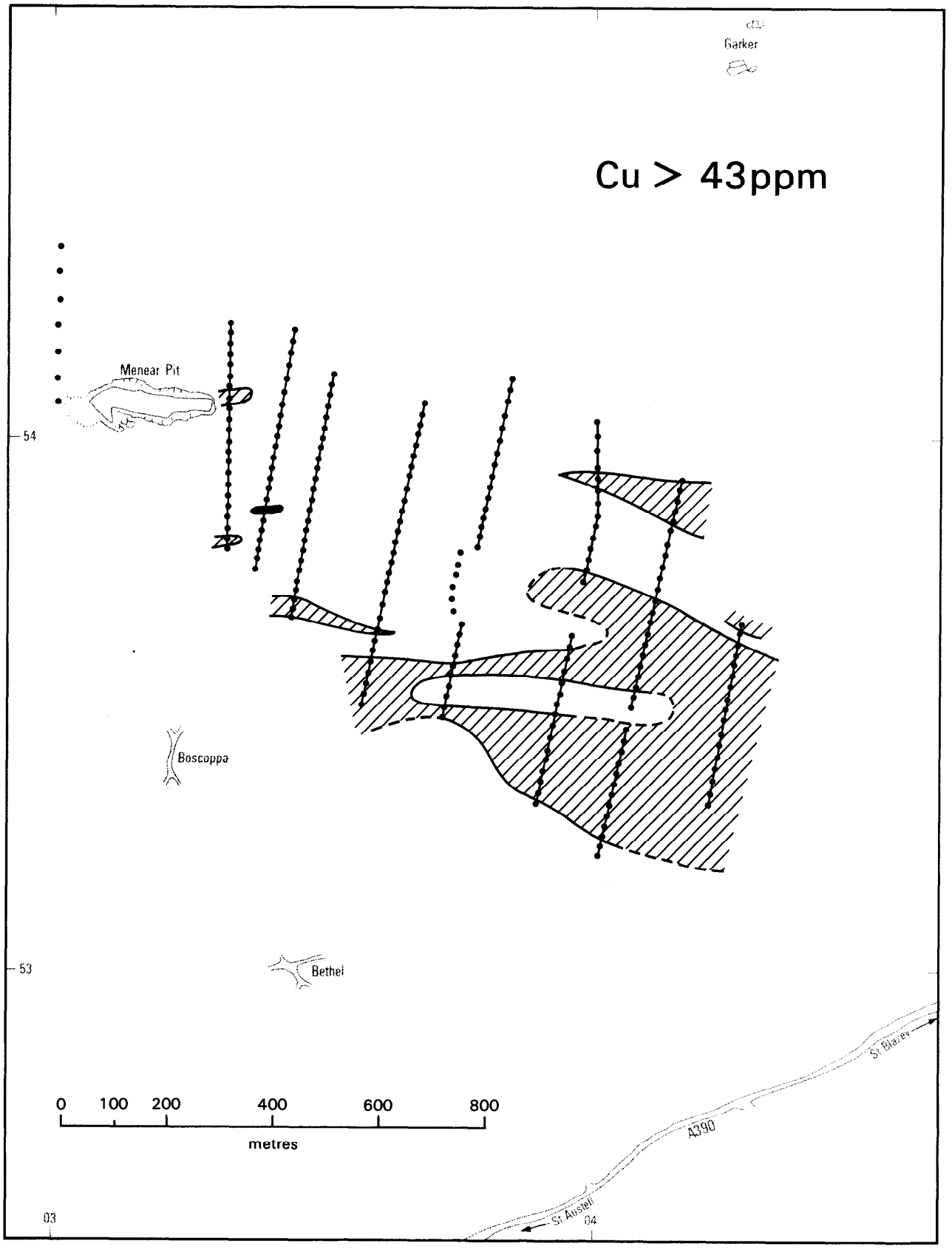

Figure 14 Distribution of copper anomalies

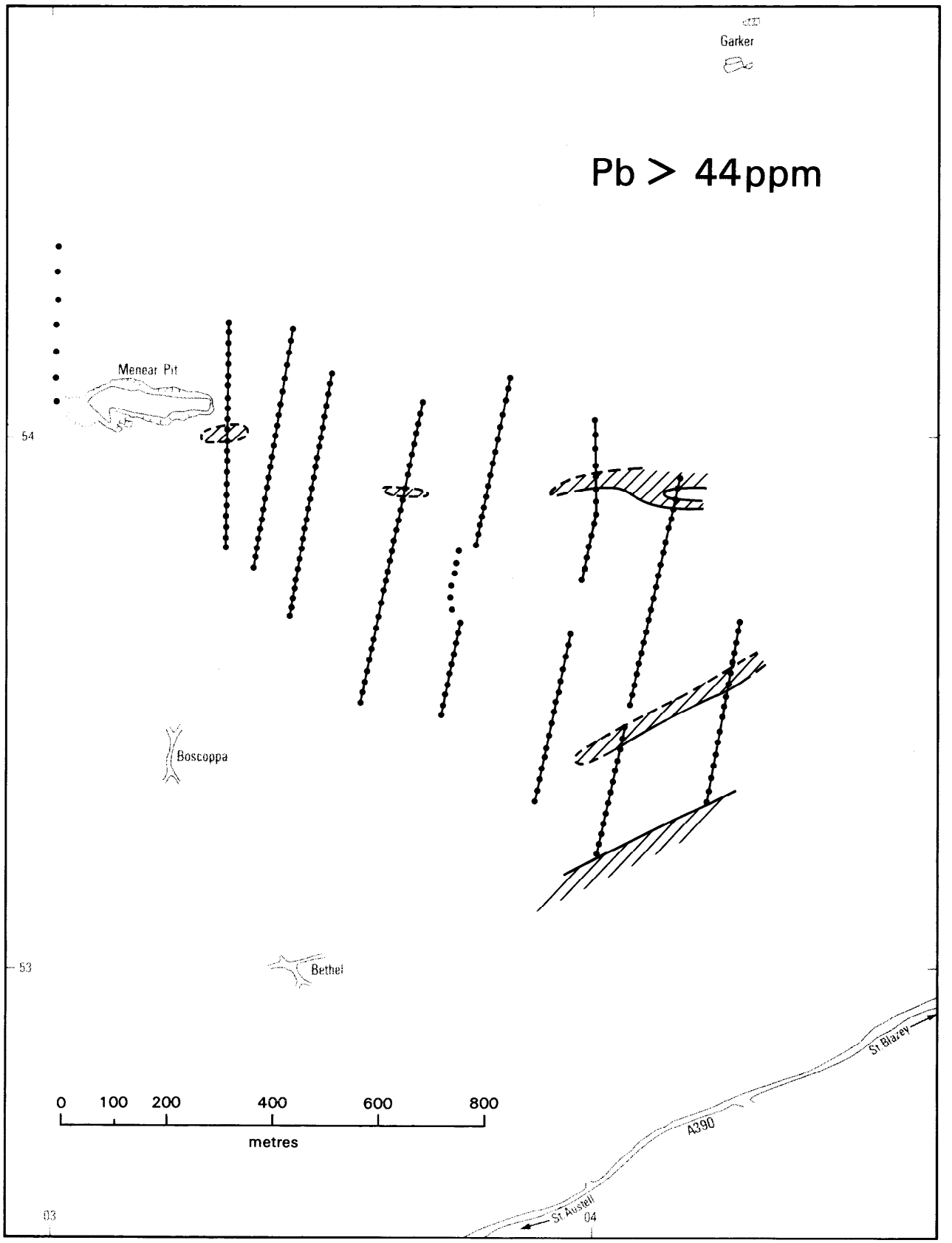

Figure 15 Distribution of lead anomalies

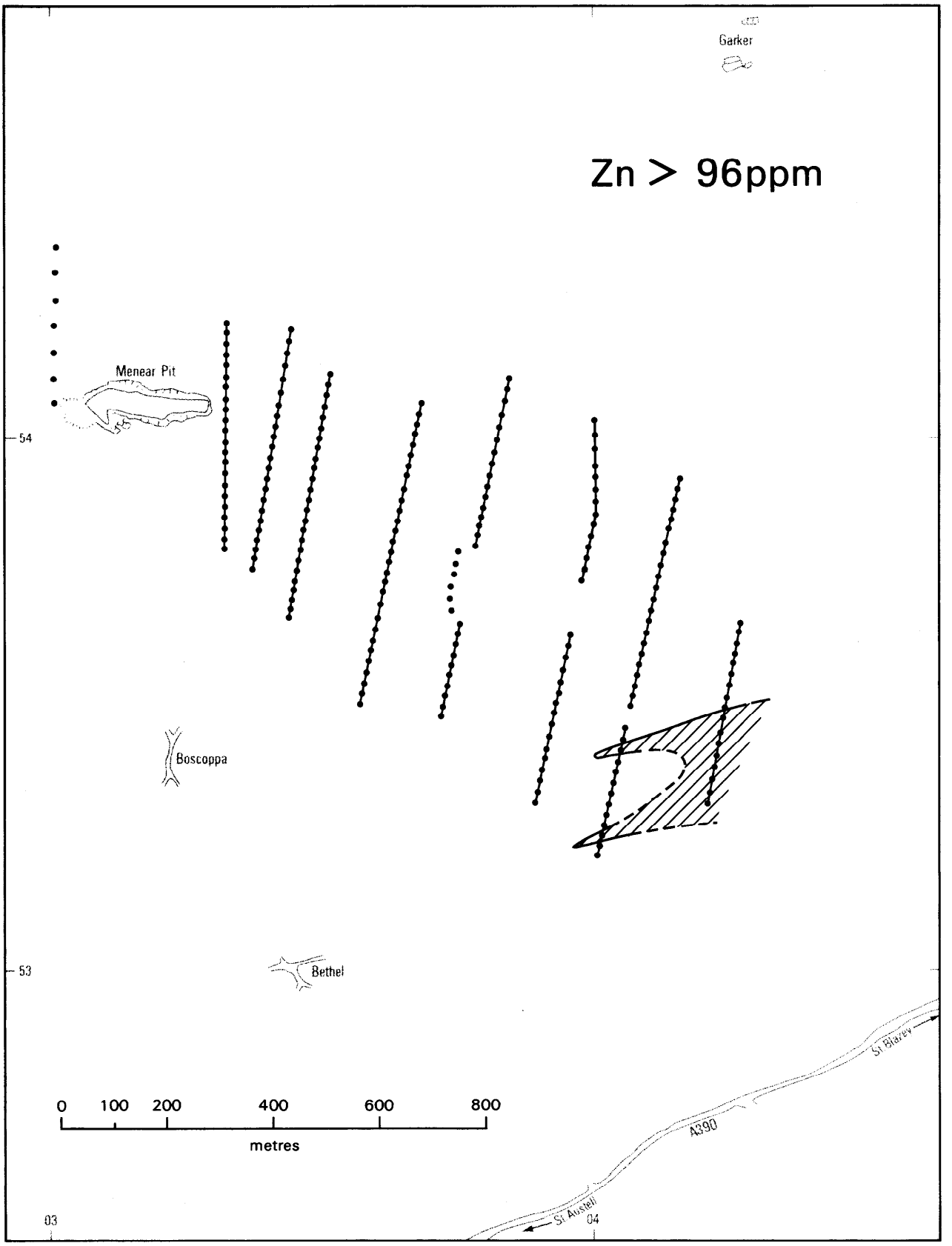

Figure 16 Distribution of zinc anomalies

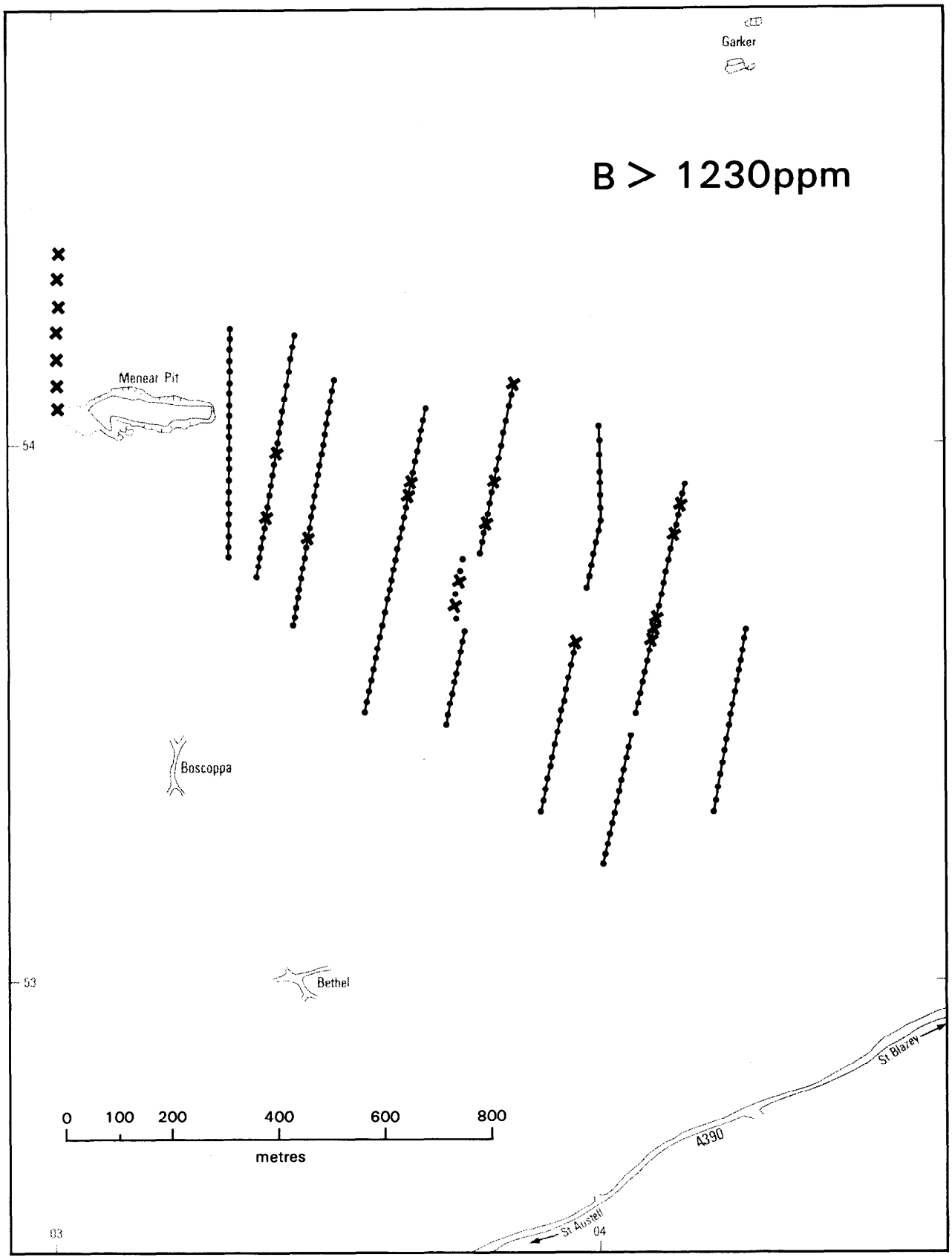

Figure 17 Distribution of boron anomalies

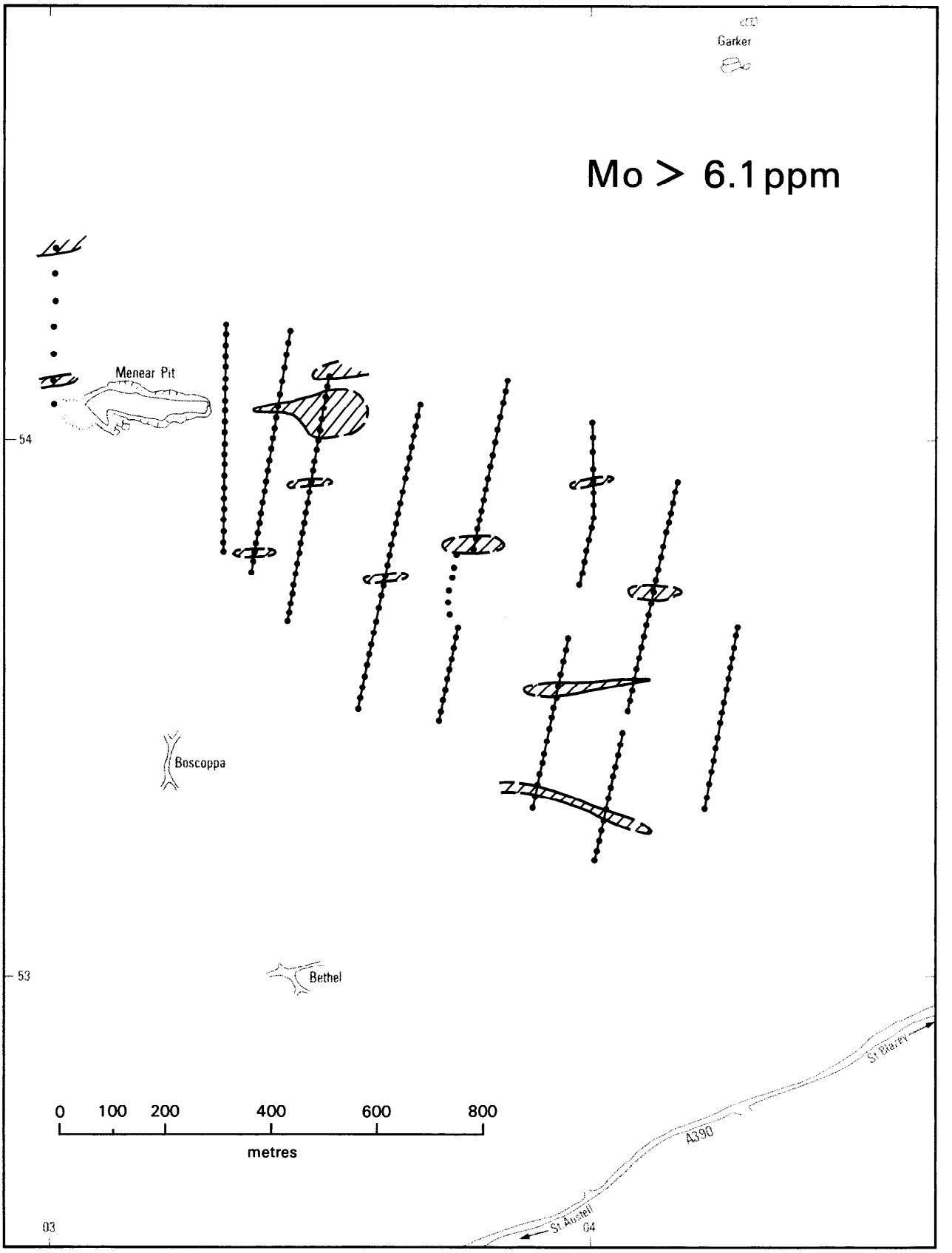

Figure 18 Distribution of molybdenum anomalies

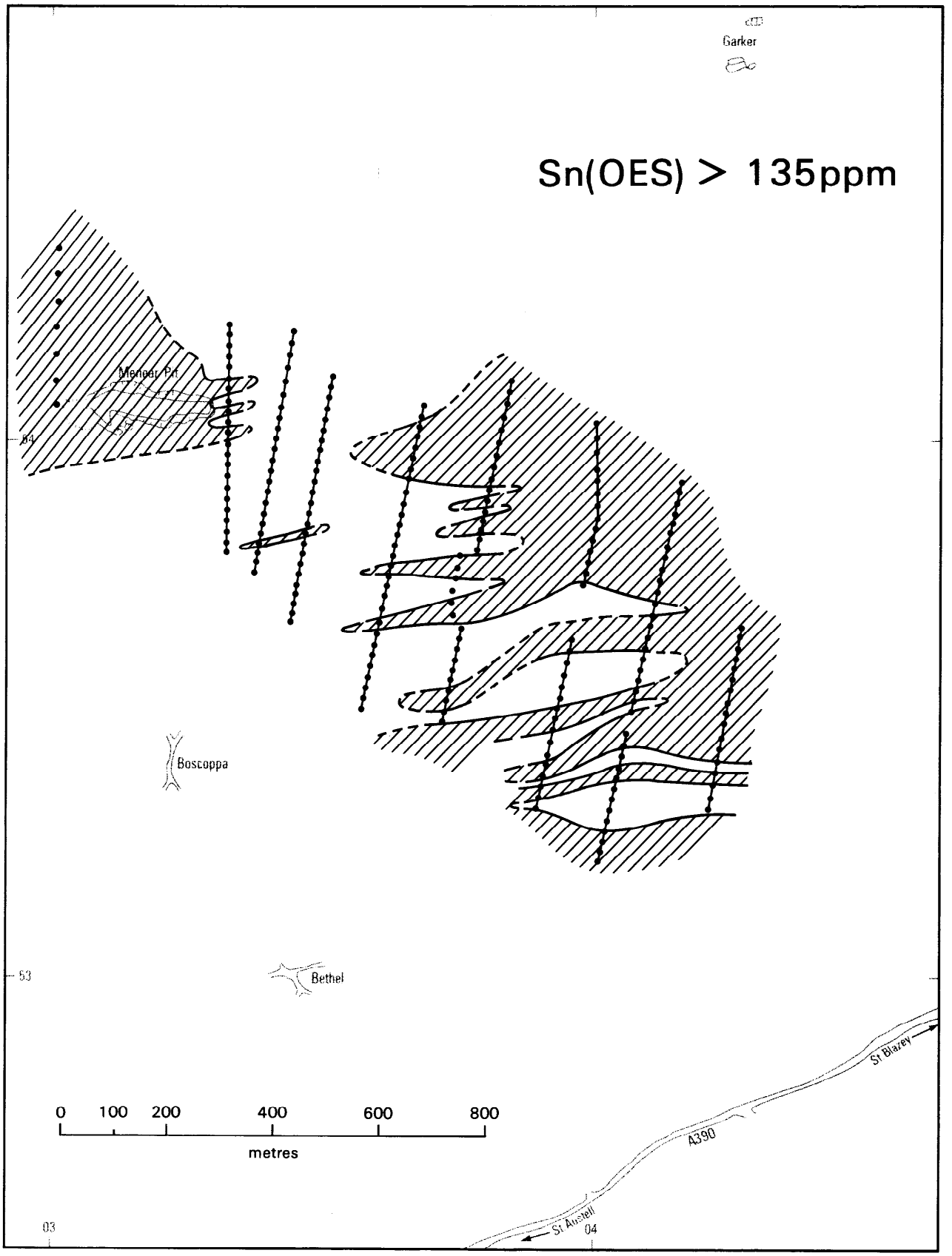

Figure 19 Distribution of tin (OES) anomalies

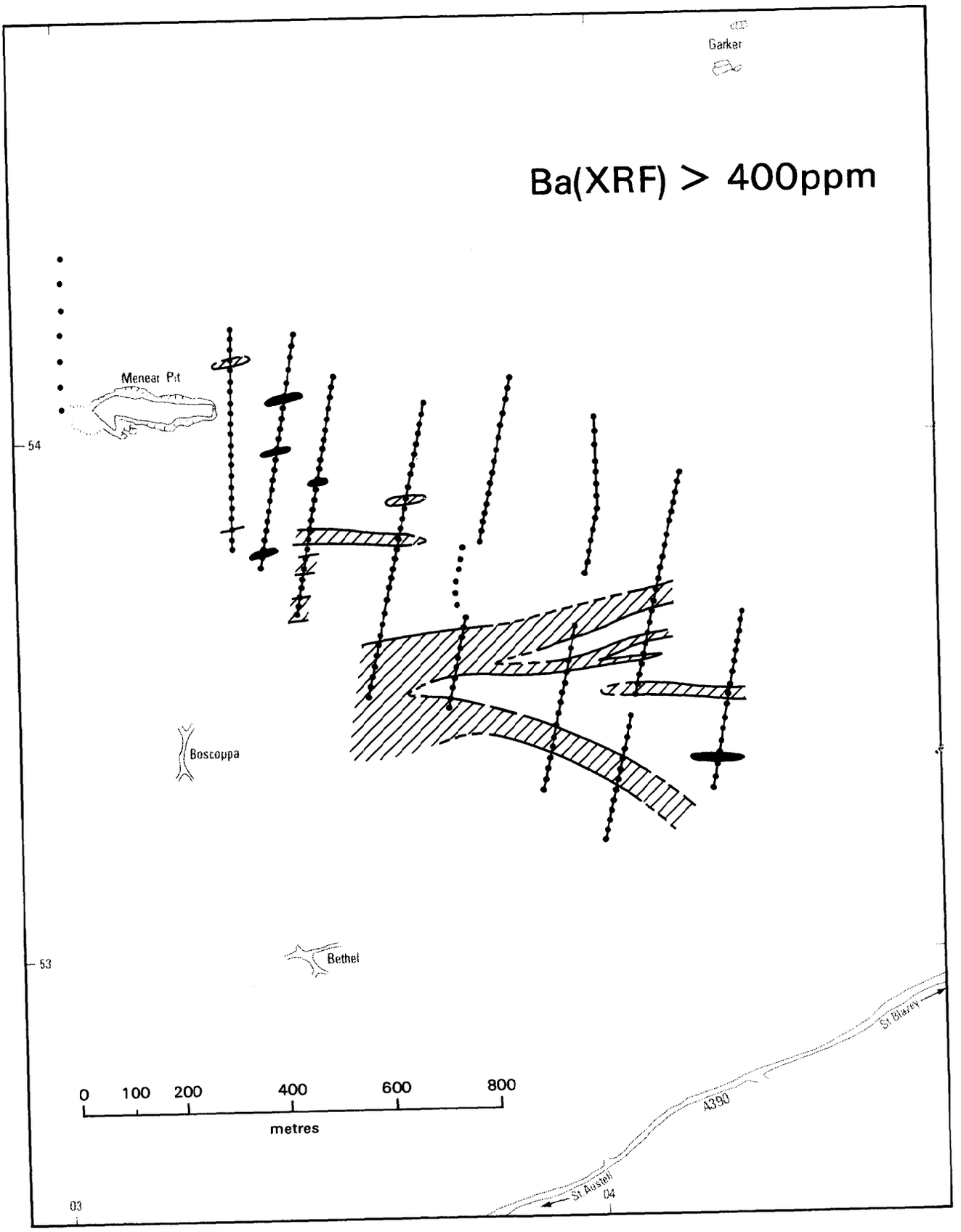

Figure 20 Distribution of barium anomalies

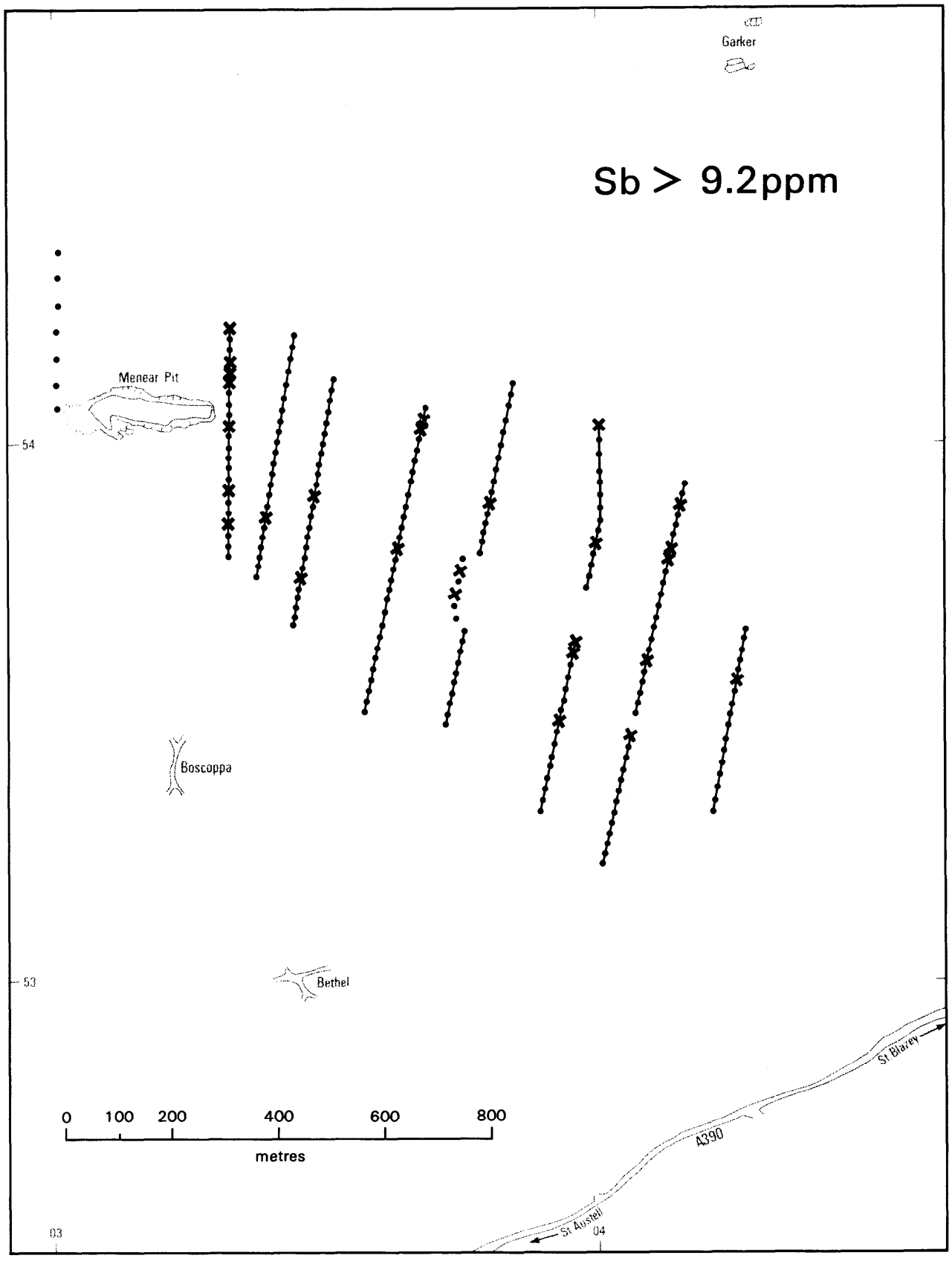

Figure 21 Distribution of antimony anomalies

Figure 22 Distribution of tin (XRF) anomalies

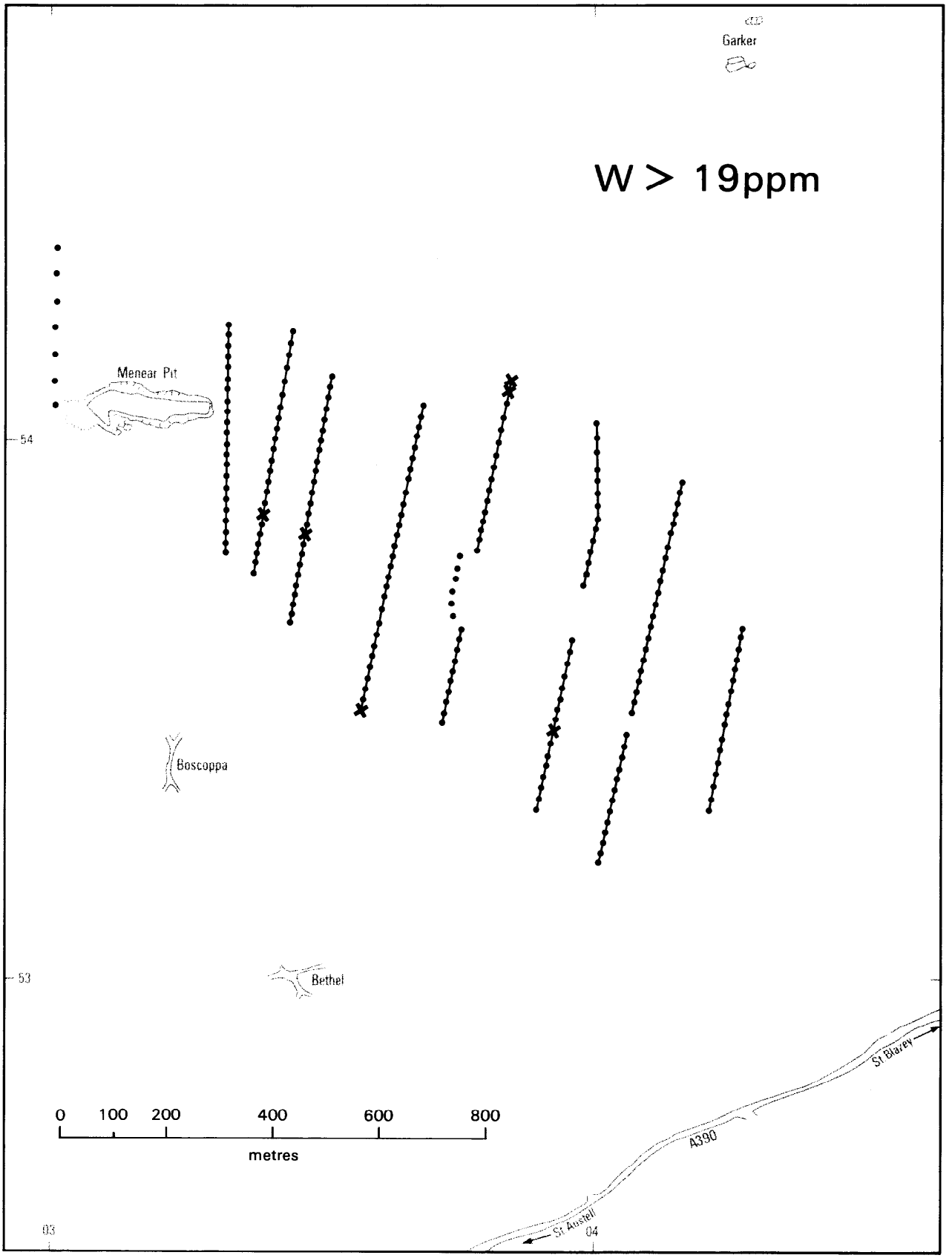

Figure 23 Distribution of tungsten anomalies

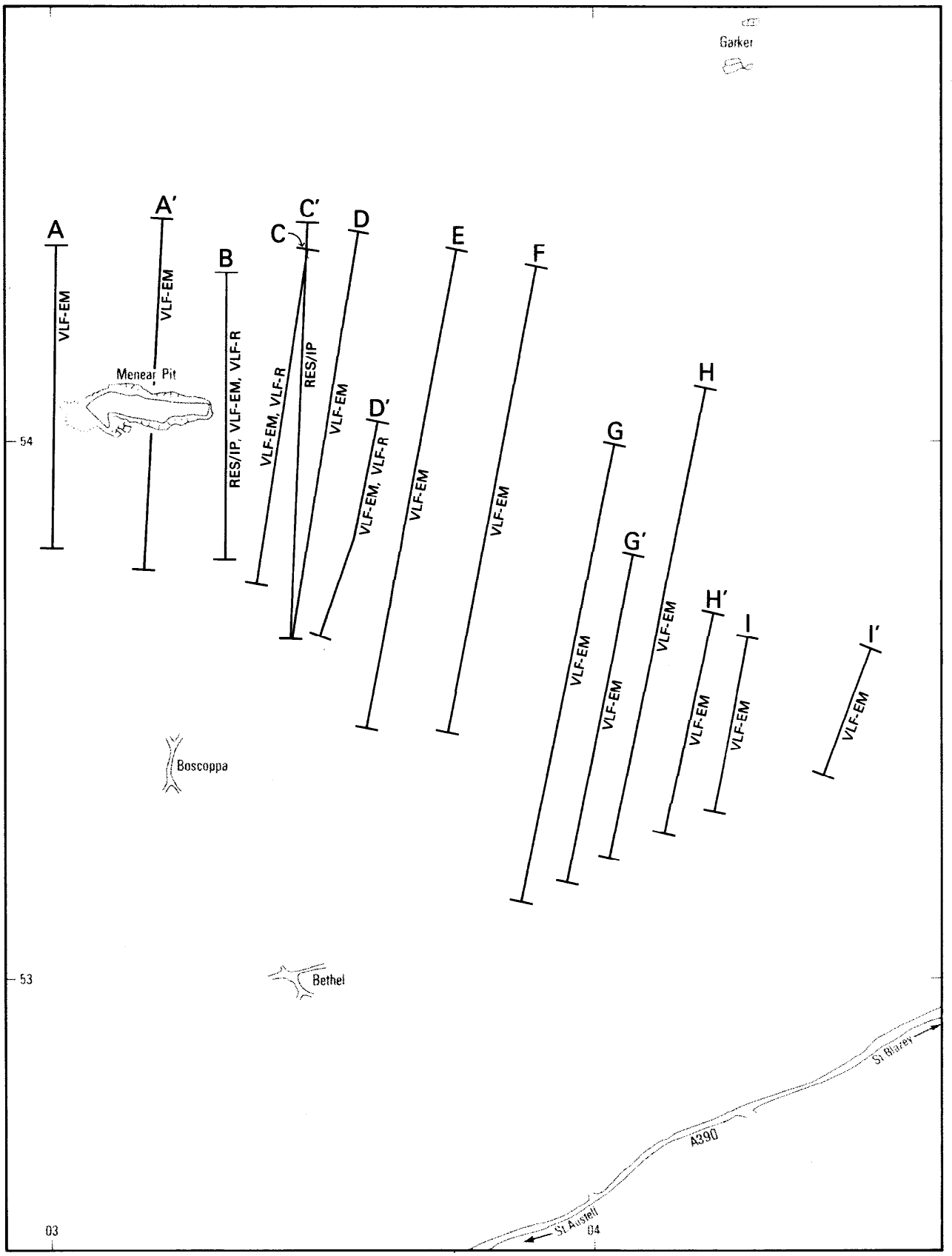

Figure 24 Geophysical traverse lines and methods employed

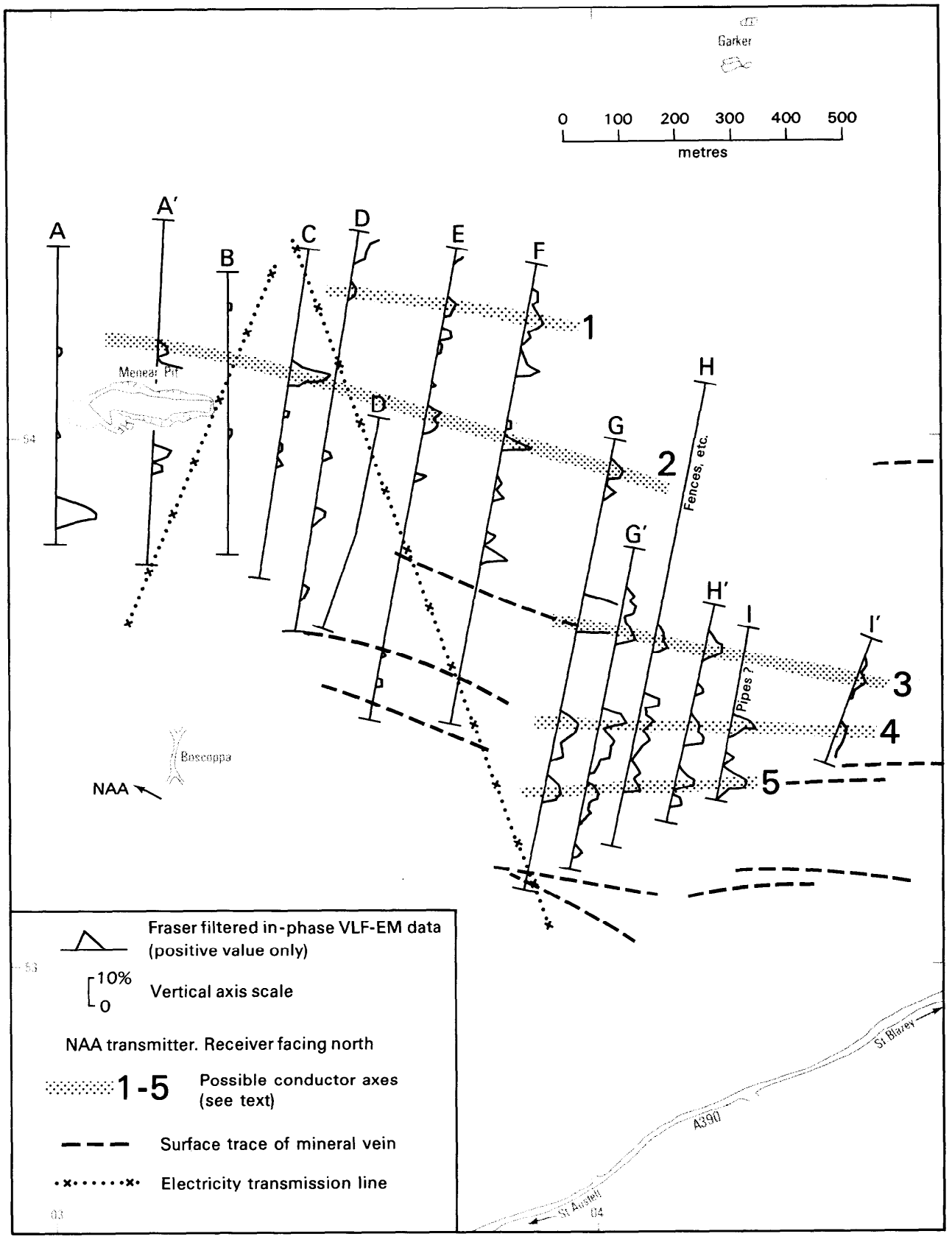

Figure 25 Fraser filtered in-phase VLF-EM data

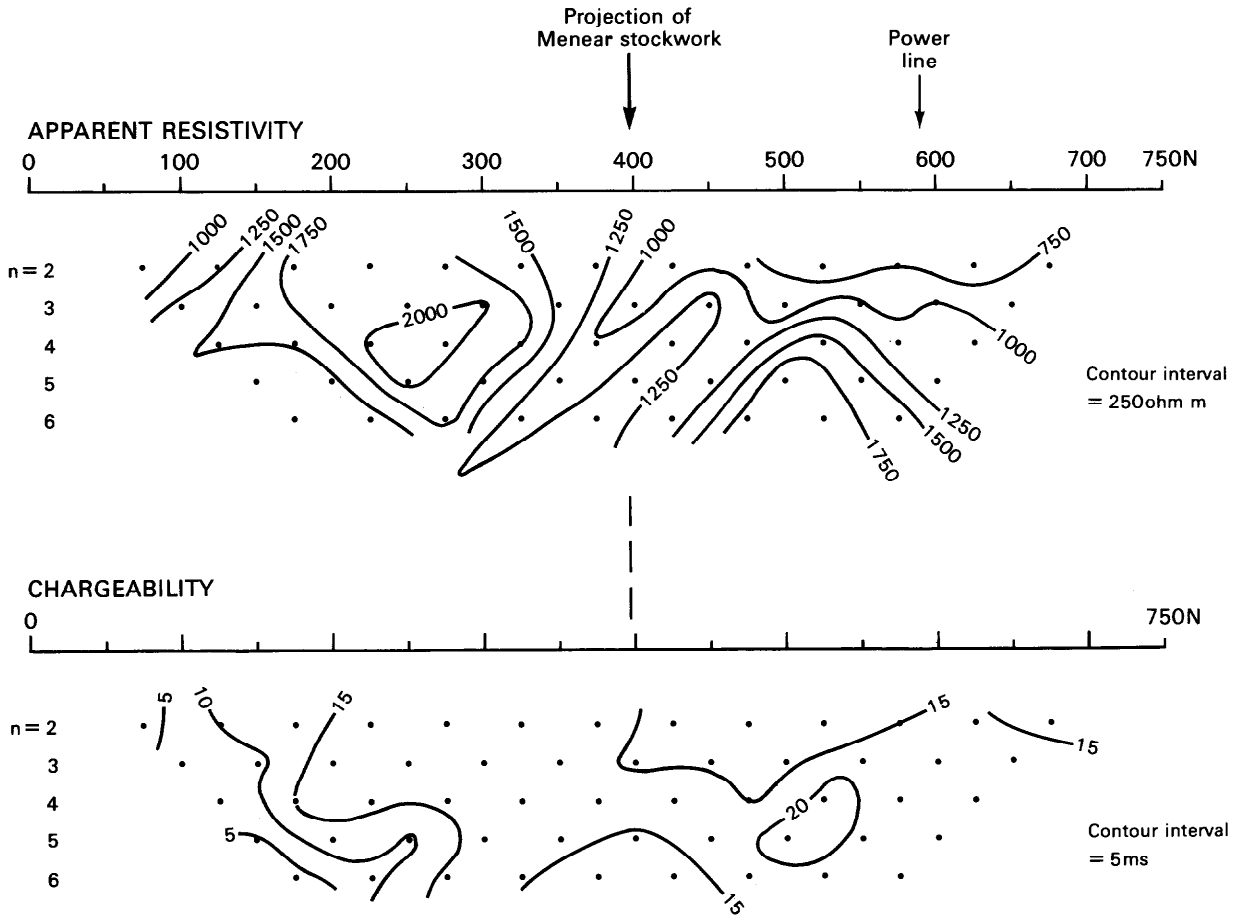

Figure 26 Resistivity and IP data for line C'

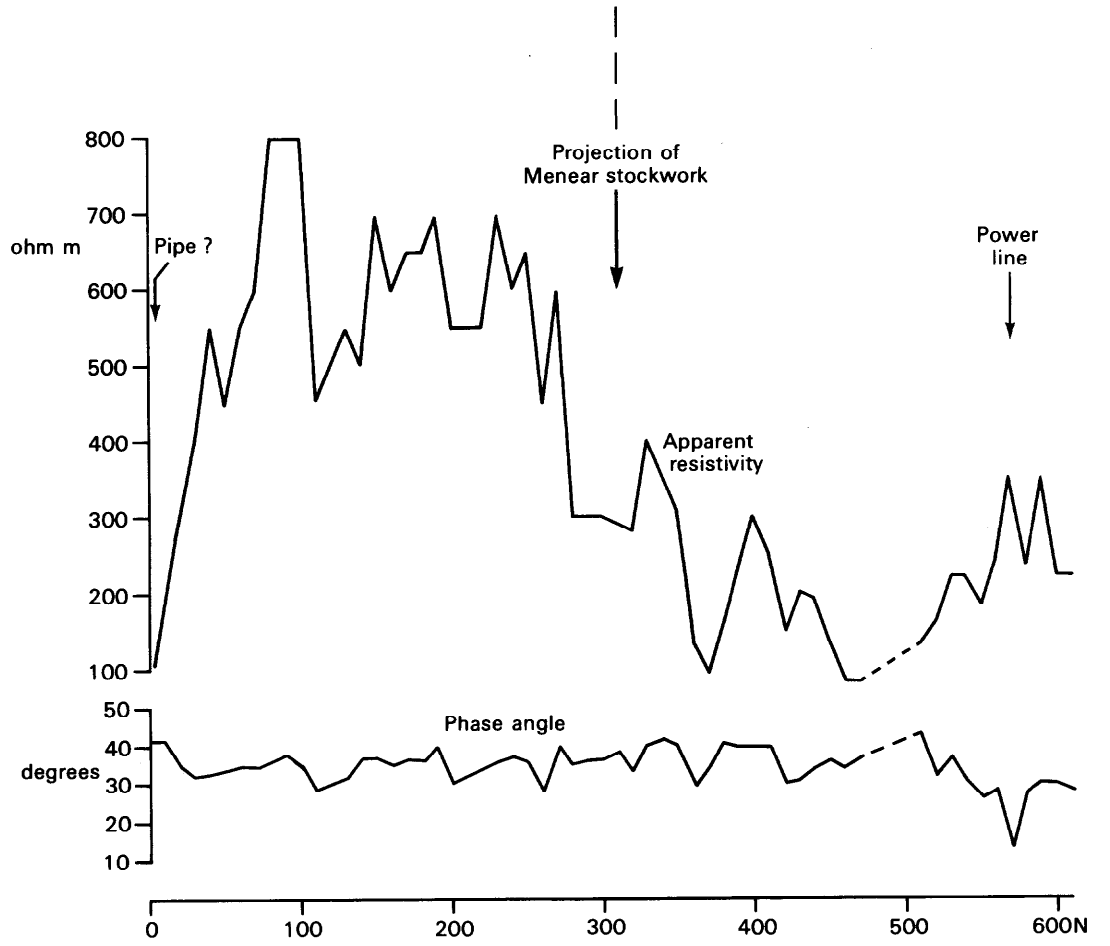

Figure 27 VLF-R data for line C